THE AMERICAN MINERALOGIST, VOL. 51, NOVEMBER–DECEMBER, 1966

MINERALOGY OF THE LABRIEVILLE ANORTHOSITE, QUEBEC

ALFRED T. ANDERSON, JR.,[1] *The Enrico Fermi Institute for Nuclear Studies and the Department of Geophysical Sciences, The University of Chicago.*

ABSTRACT

The Labrieville anorthosite massif is an example of crystallization differentiation in a plutonic environment. As in other St. Urbain-type anorthosites (characterized in particular by andesine anti-perthite and hemo-ilmenite), the lithologic sequence is: anorthosite (earliest), gabbroic anorthosite, iron-titanium oxide-rich gabbro and syenite (latest). In this sequence the following trends are observed: antiperthites become enriched in BaO/K_2O by a factor of 2, magnetites become impoverished in V_2O_3/Fe_2O_3 by a factor of 0.5, hemo-ilmenites become enriched in MnO/FeO by a factor of 4.3, pyroxenes decrease in Mg/Mg +Fe by a factor of 0.5, and apatites become enriched in Cl/F, Ce/Y and Eu/Yb. These changes are associated with a progressive decrease in the Fe_2O_3 content of the (hemo-) ilmenites from 34 per cent in anorthosite to 6 per cent in oxide-rich gabbro and syenite, indicating that the residual liquids became highly reducing relative to temperature: 1) oxygen fugacity cooling curves for isocompositional ferrian ilmenites, 2) water of constant bulk composition (or constant H_2/H_2O ratio) and 3) isocompositional titaniferous magnetites.

The Fe_2O_3 content of hemo-ilmenite in a massive hemo-ilmenite deposit (about 25 per cent) indicates that the deposit formed at a relatively early stage of the differentiation. The deposit contains appreciable corundum, whereas pockets of quartz, perthite and pyrite occur in the anorthosite, requiring physical isolation of the deposit from the anorthosite and subsequent crystallization differentiation of both, which implies that separation occurred by means of silicate liquid—iron-titanium oxide liquid immiscibility.

The 2.0 per mil deduced primary fractionation of oxygen isotopes between ilmenite and plagioclase indicates that separation of iron-titanium oxides from silicates occurred at a temperature near or above 1100° C. The biotite compositions limit the lowest crystallization temperature to a value greater than 880° C. and the highest water fugacity to a value less than 2000 bars at the late oxide-rich gabbro stage.

Analysis of the changes in the compositions of the minerals in the Labrieville massif in terms of published data on the Skaergaard intrusion (Wager and Mitchell, 1951) and the Rayleigh distillation equation reveals that the Labrieville feldspars are more than 75 per cent perfectly fractionated and that residual liquids became enriched in iron-titanium oxide and pyroxene components relative to feldspar components. According to these arguments, the earliest *liquid* evident from the Labrieville data consisted of at least 84 per cent feldspar constituents and was characterized by a water fugacity of less than 500 bars.

INTRODUCTION

About a generation ago Daly (1933) and Buddington (1939) pointed out several major differences between Precambrian domical anorthosites and the anorthosite layers of stratiform basic intrusions: Domical anorthosites are large plutons comprised of predominant very coarse-grained

[1] Present address: U. S. Geological Survey, Washington, D. C.

anorthosite and subordinate amounts of gabbroic anorthosite (10 to 22-½ per cent dark minerals) and anorthositic gabbro (22-½ to 35 per cent dark minerals). A survey of published information reveals that the plagioclases of St. Urbain type domical anorthosites (Anderson and Morin, 1964), the best known of which is the Adirondack anorthosite, are more sodic and potassic than those of all but the very latest differentiates of stratiform intrusions; also hemo-ilmenite is the dominant iron-titanium oxide mineral in St. Urbain type anorthosites, whereas titaniferous magnetite is the principal oxide mineral in layered basic intrusions.

Goldschmidt (1958, p. 152), following Kolderup, emphasized the importance of the compositions of the feldspars of domical anorthosites and related rocks: "Their gabbroid members are characterized . . . by very early potash feldspar. This feldspar has often formed solid solutions with plagioclases of andesine or oligoclase composition giving very characteristic antiperthites and perthites." Goldschmidt added that the potassium feldspar characteristically forms contemporaneously with andesine plagioclase feldspar. Goldschmidt contrasted these attributes with those of potassium poor granodiorites and trondjemites and suggested that the instability of biotite in the (presumed anhydrous) parent magma of domical anorthosites and later differentiates could account for their less siliceous but more potassic nature.

Domical anorthosites and their differentiates are distinct, therefore, from both layered basic intrusions and rocks of the granodiorite succession.

The major purpose of this investigation has been to elucidate the nature of the primary magma of a small St. Urbain type domical anorthosite and its differentiation and cooling (recrystallization) history in terms of temperature, oxygen fugacity and the ternary feldspar system by means of chemical mineralogy.

A mineralogic rather than a lithologic approach has been used throughout this study and will also be adhered to in the following presentation. This approach is chosen because it is easier to relate crystal-liquid fractionation and phase equilibrium studies to cryptic compositional changes of constituent minerals than to lithologic or modal variations.

Terminology

The meaning of the word "plagioclase" is restricted to an optically homogenous feldspar in the usual sense. "Antiperthite" denotes a feldspar intergrowth in which plagioclase is the predominant (host) phase and potassium feldspar is the subordinate (guest) phase. "Mesoperthite" describes a feldspar intergrowth in which plagioclase and potassium feldspar phases are of approximately equal abundance. Some discussion concerns

the potassium feldspar occurring as the guest phase in antiperthite. This feldspar is called "orthoclase occurring in antiperthite." It is hoped that it will be clear to the reader that by this is meant the actual potassium feldspar phase in the antiperthites and not the potassium feldspar component occurring in solid solution in the various feldspar phases.

The terminology of the iron-titanium oxide minerals is that suggested by Buddington *et al.* (1963, p. 140). In addition the expression "(hemo-) ilmenite" is introduced to denote collectively hemo-ilmenite[1] and/or ferrian ilmenite.

Geologic Setting

The Labrieville anorthosite massif is near the southeast margin of the Lake St. John (labradorite) anorthosite in a terrain of regionally metamorphosed amphibolite grade rocks in which biotite-hornblende-microcline granitic gneisses predominate. However, the massif is surrounded by a halo of biotite-poor, plagioclase-rich, hypersthene and orthoclase gneisses of approximate quartz diorite composition. Rocks of granite composition (*sensu-stricto*) are rare within about one km of the anorthosite, farther away locally discordant lenses of granitic gneiss are present, but at distances exceeding about ten km granite gneiss is generally conformable with other types of gneiss. Within several hundred meters of the anorthosite, zircons are commonly overgrown, and within about ten meters of the anorthosite, mafic quartz diorite gneiss is anomalously rich in zircon. Hemo-ilmenite in the gneiss is common within about a kilometer of the anorthosite, bur farther away its place is taken by ferrian ilmenite.

General Petrology

The field relations, rock types, and mineralogy of the Labrieville anorthosite are similar to those of the following massifs: the St. Urbain (Baie St. Paul) massif (Mawdsley, 1927), the Adirondack massif (Buddington, 1939), the Egersund massif (Michot, 1939) and the Allard Lake massif (Hargraves, 1962). For field and petrographic details the reader is referred to these descriptions and to the original work of Morin on the Labrieville anorthosite (Morin, 1956) as well as to the geologic report to be published by Quebec (Morin, *et al.* in prep.).

A diagrammatic map of the Labrieville anorthosite massif is shown in Fig. 1. There are three structural facies:

1) a domical core facies comprised primarily of strongly foliated anorthosite, 2) a surrounding border facies a few hundred meters thick composed mostly of weakly foliated, gabbroic

[1] An exsolution intergrowth of hematite in ilmenite.

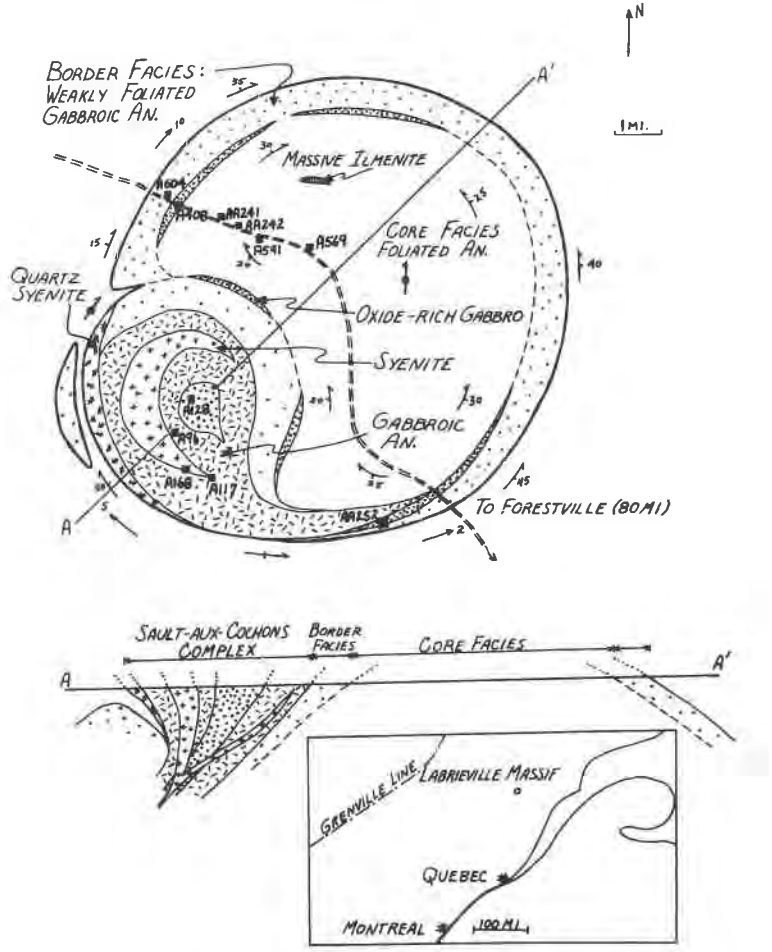

FIG. 1. Diagrammatic plan and cross-section of the Labrieville anorthosite massif, showing sample localities.

anorthosite, and 3) the funnel-shaped Sault-aux-Cochon complex made up of massive gabbroic anorthosite, anorthosite, oxide-rich gabbro and syenite.

As is the case in other St. Urbain type anorthosite masses, field relationships suggest a lithologic sequence starting with anorthosite (oldest) and continuing through gabbroic anorthosite to oxide-rich gabbro. Syenites in the Sault-aux-Cochon complex are here regarded as the latest igneous rocks of the Labrieville anorthosite massif.

The contact relationships between the marginal gabbroic anorthosite and the gneissic envelope are exposed in several places. In general the

contact is blurred over a few meters, and the affinities of the observed rock types cannot be unambiguously assigned, but along the southern margin of the Sault-aux-Cochon complex fine-grained, porphyritic gabbroic anorthosite is in sharp contact with both syenite and gneiss.

A massive hemo-ilmenite deposit is located in the core facies anorthosite. It is a tabular body about 50 m thick which dips gently, approximately parallel to the attitude of the surrounding foliated anorthosite. Apatite-rich ilmenitite occurs as a local capping over the massive hemo-ilmenite. Small pods and lenses of massive ilmenite of the order of several meters in maximum extent are particularly common in the nearby anorthosite. The smaller lenses are in sharp but irregular contact with the surrounding anorthosite, and similar contact relationships characterize the main deposit. Although fragments of anorthosite occur in the deposit, dispersed crystals of antiperthite are rare, the principal transparent minerals besides apatite are corundum, sillimanite, calcite and siderite.

Xenoliths of labradorite anorthosite occur in the rocks of the Labrieville massif. The xenoliths are sharply bounded: the plagioclase composition of one xenolith (sample AA242) changes from An 55 to An 38 over a few millimeters. Xenoliths of gneiss are common in syenite but rare in anorthosite and gabbroic anorthosite.

Labradorite metagabros occur in the surrounding gneisses and as xenoliths in the Labrieville massif. The metagabbros have variable proportions of ilmenite, magnetite, olivine, orthopyroxene, amphibole, garnet, spinel and biotite in addition to plagioclase.

Petrographic Summary

The most abundant mineral in nearly all of the rocks of the massif is antiperthite; for the most part dark minerals occur in interstitial aggregates. In the foliated rocks of the core and border facies the dark mineral aggregates are lens shaped and their preferred orientation defines the foliation. The mineralogy and abundance of the aggregates of dark minerals vary in such a way as to delimit compositional layers several centimeters to several meters thick. In contrast to the core and border facies foliated rocks, the massive rocks of the Sault-aux-Cochon complex contain dark mineral aggregates which are in subophitic relationship to antiperthite. With the exception of rare instances of tabular orthopyroxene, all dark minerals are anhedral and interstitial to feldspar in all rocks of all facies of the massif; specifically: there are no structures or textures reminiscent of gravitational accumulation of any mineral other than feldspar.

As a guide to the mineralogic make-up of the various rock types of the massif, several modes are presented in Table 1.

TABLE 1. MODES OF LABRIEVILLE ROCKS

	A96	A117	A128	A168	AA252	A408	A569	A591	A604	L31	B11-92	B11-131.5	B11-1665	B11-152	B11-156.5	B13-77
Plagioclase+ Antiperthite	80	2	45	x	52	54	85	98	91	60	n.f.	tr.	tr.	15[1]	tr.	n.f.
Potassium Feldspar	x	85	tr.	77	18	x	x	x	x	14	n.f.	n.f.	x	?	?	n.f.
Orthopyroxene	3	4	13	8	7	7	12	1	2	7	tr.	n.f.	n.f.	n.f.	n.f.	n.f.
Clinopyroxene	7	6	20	6	12	13	x	x	4	9	n.f.	n.f.	n.f.	n.f.	n.f.	n.f.
Biotite	0.3	n.f.	0.2	n.f.	n.f.	1	0.2	0.1	0.1	n.f.	tr.	n.f.	tr.	?	?	?
Ilmenite	5	1	5	3	3	20	0.4	0.7	0.8	3	52	65	94	80	98	98
Magnitite	3	2	15	3	6	6	0.1	x	0.8	6	x	tr.	n.f.	?	n.f.	x
Rutile	n.f.	n.f.	tr.	n.f.	n.f.	n.f.	n.f.	n.f.	n.f.	n.f.	tr.	?	?	n.f.	n.f.	?
Spinel	x	x	x	x	x	x	x	n.f.	x	n.f.	2	1	2	tr.	2	1
Pyrite	tr.	tr.	tr.	tr.	tr.	tr.	tr.	tr.	tr.	n.f.	3	2	tr.	n.f.	tr.	n.f.
Pyrrhotite	?	?	?	?	?	tr.	tr.	?	tr.	n.f.	?	?	tr.	n.f.	n.f.	n.f.
Corundum	n.f.	n.f.	n.f.	n.f.	n.f.	n.f.	n.f.	n.f.	n.f.	n.f.	tr.	n.f.	1	n.f.	n.f.	tr.
Quartz	tr.	tr.	tr.	1	tr.	tr.	tr.	n.f.	tr.	n.f.	n.f.	n.f.	n.f.	n.f.	n.f.	n.f.
Zircon	tr.	tr.	tr.	tr.	tr.	tr.	n.f.	n.f.	n.f.	n.f.	tr.	n.f.	tr.	n.f.	?	tr.
Calcite	tr.	n.f.	?	n.f.	n.f.	tr.	n.f.	n.f.	tr.	n.f.	tr.	tr.	tr.	tr.	tr.	tr.
Ankerite	n.f.	n.f.	n.f.	n.f.	n.f.	?	n.f.	n.f.	n.f.	n.f.	tr.	?	?	?	?	?
Siderite	n.f.	n.f.	n.f.	n.f.	n.f.	tr.	n.f.	n.f.	n.f.	n.f.	tr.	?	?	?	?	?
Apatite	1	tr.	2	2	2	4	0.8	0.2	1	1	43	32	1	5	tr.	tr.
OP	0.20	0.2	0.07		0.11	0.3		0.10								

x = Exsolution product only.
tr. = Trace.
? = Not positively identified.
n.f. = Not found.
OP = Volume per cent Opaque inclusions in feldspar megacrysts.
[1] Includes 13% Sillimanite.

The petrographic data are summarized below:

(*a*) Feldspar. The rocks of the Labrieville massif contain three varieties of feldspar megacrysts and matrix feldspar. The most prevalent feldspar megacryst is of antiperthite. Orthoclase occurring in antiperthite lacks grid twinning and has $2V = -55$ to $60°$. The second kind of feldspar megacryst is of sodic andesine and possesses a dark, vitreous appearance in hand specimen. Mesoperthite megacrysts comprise the third group of feldspar megacrysts. Antiperthite megacrysts are restricted to anorthosite, gabbroic anorthosite and oxide-rich gabbro; mesoperthite metacrysts are limited to the rare rock, syeno-gabbro and syenite. The megacrysts range in size from several millimeters to several tens of centimeters in maximum dimension.

The relatively finer-grained matrix feldspar of all of the rocks is rather similar to that of the megacrysts.

Feldspar megacrysts in all structural facies contain rodlets and platelets of hemo-ilmenite or ilmeno-hematite up to a few tens of microns in diameter or width (Fig. 3). The amount of opaque inclusions in the various megacrysts are given in table 1.

(*b*) (Hemo-) ilmenite occurs as irregular grains associated with other dark minerals in all rocks and facies. In addition to hematite and ilmenite, the hemo-ilmenites also contain occasional lamellae of magnetite.

Wherever hemo-ilmenite is adjacent to ilmeno-magnetite, a relict zoning is observed: the hematite lamellae of the hemo-ilmenite become gradually thinner and less continuous and finally disappear altogether as the contact with the ilmeno-magnetite is approached. No relict zoning exists adjacent to any of the silicates. In addition there is, in many cases, an irregular and thin zone of spinel immediately to the hemo-ilmenite side of the grain boundary with ilmenomagnetite.

In some core facies rocks there is an apparent relationship between the bulk composition of the hemo-ilmenite and its grain size. Grains smaller than about 0.2 mm in diameter are usually richer in hematite; and in many cases they are ilmeno-hematite.

(*c*) Ilmeno-magnetite. The ilmenite lamellae in the ilmeno-magnetites are 5 to 20 microns wide and are widest in the core and border facies. Spinel occurs within the ilmenite lamellae in patches and also as independent lamellae ($n = 1.783$) in the ilmeno-magnetites.

There is less than 0.1 per cent ilmeno-magnetite in noritic anorthosite (sample A569) of the core facies. Where observed it is associated with orthopyroxene and hemo-ilmenite, but not necessarily with quartz.

In the massive hemo-ilmenite deposit, magnetite is similarly rare and occurs primarily as lamellae in hemo-ilmenite and as small grains associated with pyrite.

(*d*) Pyroxenes. Orthopyroxene is common to all rocks and facies and generally has exsolution lamellae of clinopyroxene parallel to (100), but in some oxide-rich gabbro and syenite some grains have exsolution lamellae parallel to the (001) plane of a monoclinic ancestor.

Clinopyroxene is rare in core facies where its presence may be due to recrystallization after exsolution from orthopyroxene. Its abundance increases in gabbroic anorthosite, oxide-rich gabbro and syenite where it is commonly schillered by opaque platelets and may contain fine exsolution lamellae of orthopyroxene.

Other minerals. Biotite is a minor, but ubiquitous, constituent of all rocks except syeno-gabbro and syenite in which it is altogether absent.

Apatite is another minor, but ubiquitous, constituent of all rocks. It is particularly abundant in the oxide-rich gabbros and in the massive ilmenite deposit.

Pyrite is present in very minor amounts and is typically associated with the iron-titanium oxides and other sulfides, namely chalcopyrite and pyrrhotite.

Zircon is common as irregular grains associated with ilmeno-magnetite and hemo-

ilmenite in the oxide-rich gabbros. It is also present in some gabbroic anorthosites of the Sault-aux-Cochon complex. Stout crystals of euhedral zircon occur together with minor amounts of anhedral zircon in the syenites.

Rutile is of rare occurrence in some oxide-rich gabbros and in the massive ilmenite deposit.

Quartz was identified in all of the major feldspathic rock types. Small amounts are associated with the aggregates of dark minerals, especially orthopyroxene; quartz is abundant only in rare, isolated pockets of perthite, quartz and pyrite which are surrounded by turbid feldspar, chloritized orthopyroxene, and leucoxenic ilmenite.

Calcite is the most common carbonate but is found only in certain layers in the border facies, in the oxide-rich gabbros and in the massive ilmenite deposit. Siderite is present locally and may be accompanied by ankerite.

Corundum, spinel, and sillimanite are minor minerals found only in the massive ilmenite deposit.

Analytical Methods

Feldspar, apatite, biotite, pyroxene and iron-titanium oxide mineral separates were obtained from seven rock specimens by means of heavy liquids, Frantz magnetic separator and hand picking.

Refractive index determinations. Plagioclase refractive indices were determined by a universal stage technique similar in all essential aspects to that described by Smith (in Hess, 1960). The refractive indices of the orthopyroxenes were determined by the flat stage rotation technique of Hess (1960).

Structural state determinations. The structural state parameters Gamma (Smith and Gay, 1958) and Delta (Yoder and Smith, 1956) were determined on a Norelco diffractometer at Princeton University using a spinner attachment.

Some variation in the character of the $(1\bar{3}1)$ plagioclase peak from identical samples is believed due to the irregular effect of grinding on liberating orthoclase from antiperthite. The (131) orthoclase peak and the $(1\bar{3}1)$ plagioclase peak nearly coincide in this composition range.

Chemical analyses. All feldspar, apatite and the larger iron-titanium oxide mineral separates were analyzed by Zoltan Katzendorfer and Henri Boileau at the laboratories of the Quebec Department of Natural Resources, using mostly classical methods. The smaller iron-titanium oxide mineral separates and the biotites were analyzed by Y. Chiba at the Japan Analytical Chemistry Research Institute, Tokyo, using rapid methods of analysis. The ilmeno-magnetite separated from AA252 was split and analyzed by both laboratories to provide an internal basis of comparison.

Electron microprobe analyses. Selected feldspars were analyzed for Ca, Na, K, Ba, Sr, Fe and Ti on the ARL electron microprobe at the University of Chicago using feldspar and ilmenite reference standards. The ortho and clinopyroxenes were analyzed for Ca, Mg, Fe, Mn, Al, and Ti using pyroxene, feldspar and ilmenite reference standards. The analyses were corrected for background and matrix absorption (Birks, 1963) but not for atomic number effects.

Rodlets of hemo-ilmenite and ilmeno-hematite in selected antiperthite and plagioclase megacrysts were analyzed on the electron microprobe after attempted homogenization by heating in air for about 30 hours at 850° C.

Oxygen isotope analyses. Aliquots of the analysed feldspar, apatite and iron-titanium oxide mineral separates were reacted with bromine pentafluoride at temperatures of about 475, 620 and 620° C. respectively, according to the technique described by Clayton and Mayeda (1963). The oxygen yields from the reactions were 100 per cent within about 2 per cent. The oxygen was converted to carbon dioxide and analyzed in a double-collecting Nier type mass spectrometer (Nier, 1947, McKinney *et al.*, 1950). The results are reported in (per mil).

$$\delta = \left[\frac{O^{18}/O^{16}_{\text{sample}} - O^{18}/O^{16}_{\text{standard}}}{O^{18}/O^{16}_{\text{standard}}}\right] \times 1000$$

The reported deltas were corrected for spectrometer valve mixing and C^{13}/C^{12} ratio according to the equations of Craig (1957) and are relative to the standard mean ocean water (SMOW) standard of Craig (1961). The deltas are precise relative to one another within 0.2 per mil, but their accuracy relative to SMOW depends upon the accuracy of the carbon dioxide-water fractionation determined by Compston and Epstein(1957).

Calculation Procedures. The molecular per cents of An, Ab and Or in the chemically analyzed feldspars were calculated from the reported amounts of CaO, Na_2O, and K_2O and normalized to 98.0 per cent total to make allowance for the amounts of SrO and BaO reported in A9b and A128.

The BaO/K_2O ratio for the total feldspar of A604 was calculated from the electron micro-probe analysis of the orthoclase rodlets in antiperthite and normalized to the wet chemical values of the other feldspars by using the BaO/K_2O ratio obtained by probe for the orthoclase rodlets in the antiperthite of A408 and the classically analyzed BaO/K_2O ratio of the feldspar from A408.

The molecular compositions of the analyzed (hemo-) ilmenites and ilmeno-magnetites were computed in terms of ilmenite (Il) and hematite

(Hm) and magnetite (Mt) and ulvospinel (Usp) according to the scheme outlined by Buddington and Lindsley (1964) except that they were not normalized to 100 per cent totals but left as the actual mole fractions.

The analyses of the ilmeno-magnetite from A569 and A604 were corrected for impurities (2.6% hemo-ilmenite+1.0% orthopyroxene in

TABLE 2. ANALYSES OF LABRIEVILLE FELDSPARS

	A9b	A9b[1]	A128	A128[1]	A168	AA252	A408	A569	A604
SiO_2	58.60	58.92	58.21	59.08	62.13	59.50	59.21	58.76	58.94
Al_2O_3	24.68	25.09	24.91	25.02	21.73	23.95	24.54	25.03	24.85
MgO	0.04	0.03	n.d.	0.08	n.d.	n.d.	n.d.	n.d.	n.d.
CaO	7.55	7.14	7.18	7.07	3.48	6.47	6.69	7.38	7.20
SrO	0.16	0.39	0.15	0.47	n.d.	n.d.	n.d.	n.d.	n.d.
BaO	0.11	0.11	0.13	0.13	0.39	0.14	0.11	0.07	0.07
K_2O	1.38	1.32	1.33	1.30	5.38	1.48	1.55	1.41	1.51
Na_2O	6.31	5.97	6.76	6.26	5.78	6.83	6.48	6.46	6.43
FeO	0.08	0.06	0.05	0.06	0.03	0.08	0.19	0.12	0.08
Fe_2O_3	0.23	0.24	0.23	0.24	0.31	0.030	0.23	0.07	0.16
TiO_2	0.025	0.08	0.027	0.08	0.020	0.028	0.006	0.017	0.015
MnO	0.002	0.002	0.001	0.002	n.d.	n.d.	n.d.	n.d.	n.d.
P_2O_5	0.02	0.02	0.02	0.01	0.014	0.02	0.02	0.02	0.02
V_2O_5	0.001	n.d.	0.001	n.d.	n.d.	n.d.	n.d.	n.d.	n.d.
H_2O^+	0.11	0.05	0.20	0.17	0.09	0.12	0.20	0.10	0.16
Total	99.30	99.42	99.20	99.97	99.35	98.64	99.23	99.44	99.43
$CaAl_2Si_2O_8$[2]	36.3	36.1	34.0	34.9	16.9	31.2	32.8	35.4	34.7
$SrAl_2Si_2O_8$	0.4	1.1	0.4	1.3	n.d.	n.d.	n.d.	n.d.	n.d.
$BaAl_2Si_2O_8$	0.2	0.2	0.2	0.2	0.7	0.3	0.2	0.1	0.1
$KAlSi_3O_8$	7.9	8.0	7.5	7.6	31.1	8.5	9.0	8.0	8.7
$NaAlSi_3O_8$	54.9	54.6	57.9	55.9	50.8	59.6	57.5	56.0	56.0
$100BaO/k_2O$	8.0	8.3	9.8	10.0	7.2	9.5	7.1	5.0	4.6[3]
$Fe^{3+}/Fe^{3+}+Fe^{2+}$	0.72	0.75	0.67	0.75	0.90	0.77	0.52	0.21	0.47

[1] 40–80 mesh.

[2] Molecular percents.

[3] Value believed in error: microprobe analysis of orthoclase rodlets suggests $100BaO/K_2O = 7.2$ by comparison with A408.

A569 and 8.1% hemo-ilmenite in A604) before calculating their molar compositions or their V_2O_3/Fe_2O_3 ratios and distribution coefficients.

Chiba reports r_2O_5, whereas the Quebec analysts report V_2O_3. Chiba's r_2O_5 determinations were converted to comparable V_2O_3 values by normalizing according to the ratio of V_2O_3/r_2O_5 (*i.e.* 0.5) reported by the Quebec analysts and Chiba respectively on AA252 ilmeno-magnetite.

RESULTS

(*a*) Feldspars. The standard chemical analyses of the feldspars are presented in Table 2; the electron micro-probe analyses and least refractive indices are listed in Table 3. For the most part the antiperthites have relatively consistent compositions of about An 35 Or 8, however, the

BaO/K_2O ratio of the antiperthites increases from 5.0 to 9.8 from core facies noritic anorthosite to oxide-rich gabbro in the Sault-aux-Cochon complex. Plagioclase megacrysts have slightly more variable composi-

TABLE 3. FELDSPAR MICROPOBE ANALYSES

	Ab	An	Or	Cn	SrO	Fe	Ti	Hm	nα	An
A9bP		38.7	3.2		0.25	0.081			1.5472	36.5
A9bPM	57.7	37.5	3.8		0.27	0.087	0.007	53	1.5465	35
A9bK	6.6		87.3	3.8	0.27	0.026				
A117PM		38.0	2.8							
A117PM		36.5	2.8		0.16	0.027		(12)[1]	1.5469	36
A117PM		33.0	2.8							
A117PM		28.0	2.1							
A117PM		27.5	2.5							
A117PP		22.3	0.1		0.12	0.029				
A117PP		20.2	0.3							
A117KP		0.2	91.8		0.21	0.021				
A128P		36.4	4.9		0.31	0.075			1.5475	37
A128PM	57.6	36.9	5.4		0.27	0.083	0.009	17	1.5466	35
A128K	6.2	0.7	83.7	5.1	0.39	0.021				
A168PM	56.1	38.2	2.6							
A168PP	73.5	26.8	0.2		0.11	0.050			1.5425	27
A168KP	5.8	0.2	89.8		0.22	0.017				
AA241P	61.5	36.9	2.2						1.5460	34
AA241PM	54.0	37.6	3.2					65	1.5474	37
AA241K	8.3	0.6	87.4	2.2						
AA252P	60.5	34.6	3.1							
AA252PM	56.8	39.5	4.5		0.23	0.090	0.012	38	1.5475	37
AA252PP		34.4	1.8		0.20	0.086				
AA252KP		0.2	93.8		0.30	0.032				
A408P		36.2	3.0		0.26	0.070			1.5470	36
A408PM	59.2	36.1	3.8		0.25	0.095	0.010	57	1.5468	36
A408K	6.9	0.6	89.0	3.3						
A569P	56.8	37.6	3.4		0.26	0.10			1.5466	35
A591P		36.7	3.1		0.25	0.081			1.5463	35
A591PM		36.0	3.6		0.23	0.086		(75)	1.5466	35
A591K		0.2	97.5		0.27	0.021				
A604P		37.6	3.2		0.26	0.091			1.5473	36.5
A604PM	57.3	38.3	4.1		0.25	0.080			1.5475	37
A604K	5.5		87.8	3.3	0.24	0.022				

Abbreviations: P = average plagioclase, PM = plagioclase phase of plagioclase or antiperthite megacryst, K = orthoclase occurring in antiperthite, PP = plagioclase phase of mesoperthite, KP = potassium feldspar phase of mesoperthite. Also, Hm = average mol per cent Fe_2O_3 in rhombohedral oxide inclusions in megacrysts, An deduced from the reported refractive index α according to the curve of Hess (1960).

[1] Values in parentheses visual estimates.

tions about An 38 Or 4. In particular the Or contents of plagioclase megacrysts in the oxide-rich gabbros and syeno-gabbro are greater than they are in syenite. Plagioclase megacrysts in syenite are zoned adjacent to mesoperthite rims: as the mesoperthite rim is approached, the plagioclase becomes less calcic and less potassic. The composition of the plagioclase phase in mesoperthites varies between An 20 Or 0.2 and An

34 Or 1.8. The potassium feldspar phase occurring as antiperthite and mesoperthite is rather similar in composition: about Or 90 Ab 7. The potassium feldspar in antiperthite and mesoperthite is generally slightly richer in strontium and much poorer in iron than the plagioclase associated with it.

Spot analyses were made along a profile crossing the contact between the labradorite xenolith, AA242, and its host andesine antiperthite anorthosite. The results of this profile are shown in Fig. 2; the plagioclase changes composition from An 55 to An 38 over a distance of about 3 mm, most of the change occurring on the xenolith side of xenolith-host contact as deduced from the first appearance of antiperthite.

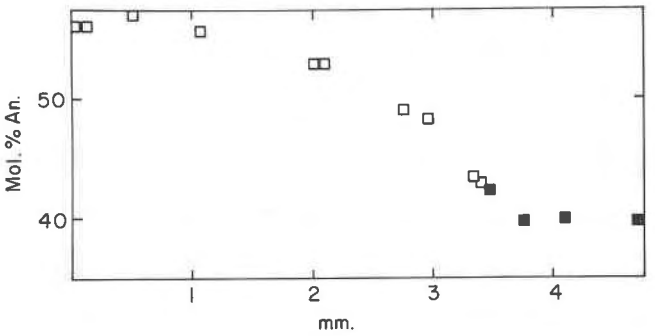

FIG. 2. The feldspar compositional variation across the contact between a labradorite anorthosite xenolith (open squares) and the andesine antiperthite host (solid squares).

Structural state parameters, Delta and Gamma, of the plagioclases are given in Table 4. All of the plagioclases are of low to low-intermediate structural state.

Two powder photographs of potassium feldspar occurring in antiperthite in the oxide-rich gabbro (A128) revealed no splitting of the (131), (130) or (111) lines. The potassium feldspar is therefore called orthoclase (Goldsmith and Laves, 1954).

(*b*) Iron-titanium oxide minerals. The standard analyses of the ilmenomagnetite and (hemo-) ilmenite separates are given in Table 5 together with the averages of the electron micro-probe analyses of the opaque inclusions in coexisting feldspar megacrysts. Compared to magnetites from quickly cooled basic igneous rocks (Buddington and Lindsley, 1963), the Labrieville magnetites have very low titanium contents. The hematite content of the Labrieville (hemo-) ilmenites varies between 34 per cent in core facies noritic anorthosite to 5 per cent in Sault-aux-Cochon oxide-rich gabbro and syenite. The average hematite content of the opaque

inclusions in feldspar megacrysts is always greater than in the coexisting (hemo-) ilmenite in the groundmass, but is related to it as shown in Fig. 3. Both the V_2O_3/Fe_2O_3 ratio of the magnetites and the MnO/FeO ratio of the ilmenites show large changes, both of which are correlated with the BaO/K_2O ratio of the antiperthites, as shown in Fig. 4.

Electron probe and oxygen isotope analysis of the ilmenite lamellae in ilmeno-magnetite from the oxide-rich gabbro, Al28, revealed that the

TABLE 4. PLAGIOCLASE STRUCTURAL STATE PARAMETERS

	Gamma	Delta	An	Or
A9bP	0.40	1.73	38.7	3.2
A9bPM	0.32	1.70	37.5	3.8
A117PM	0.40	1.74	36.5	2.8
A128P	0.43	1.75	36.4	4.9
A128PM	0.41	1.74	36.9	5.4
A168PM	0.44		38.2	2.6
AA241P	0.37	1.72	36.9	2.2
AA241PM	0.35	1.71	37.6	3.2
AA252PM	0.39	1.73	39.5	4.5
A408P	0.40	1.73	36.2	3.0
A408PM	0.44	1.75	36.1	3.8
A569P	0.39	1.73	37.6	3.4
A591P	n.d.	1.72	36.7	3.1
A591PM	0.35	1.71	36.0	3.8
A604P	0.37	1.72	37.6	3.2
A604PM	0.34	1.71	38.3	4.1

Gamma $= 2\theta(220) + 2\theta(131) - 4\theta(1\bar{3}1)$.
Delta $= 2\theta(131) - 2\theta(1\bar{3}1)$.
Abbreviations as in Tables 1–2.

lamellae have identical iron and titanium abundances and O^{18}/O^{16} ratios to those of the coexisting ilmenite.

(*c*) Pryoxenes. The electron micro-probe analyses of the coexisting pyroxenes are listed in Table 6, together with their refractive indices. The iron content of the pyroxenes increases irregularly from core facies noritic anorthosite to Sault-aux-Cochon syenite and correlates with the V_2O_3/Fe_2O_3 ratio of the magnetites as shown in Fig. 4.

(*d*) Apatites. The standard chemical analyses of the apatites are listed in Table 7. The rare earth and chlorine content of the apatites correlates with the V_2O_3/Fe_2O_3 ratio of the magnetites, Fig. 4.

(*e*) Biotites. Standard chemical analyses of the biotites are reproduced in Table 8, together with their physical properties. The contents of water plus fluorine increase from the core facies noritic anorthosite to the

TABLE 5. IRON-TITANIUM OXIDE ANALYSES

	A9b-Mt	A9b-Il	A128-Mt	A128-Il	A168-Mt[1]	A168-Il[1]	AA252-Mt	AA252-Mt[1]	AA252-Il[1]	A408-Mt-1	A408-Mt-2a	A408-Mt-2b	A408-Il	A604-Mt	A604-Il	A569-Mt[1]	A569-Il[1]	B11-131.5-Il	B11-1526-Il	B11-156.5-Il	A128-Mt
TiO_2	0.94	45.95	3.81	49.71	4.65	48.36	1.24	1.15	45.43	0.97	1.01	1.02	41.00	5.04	39.30	2.86	32.61	35.95	36.89	38.97	3.41
FeO	30.35	38.09	30.46	38.36	29.26	39.55	30.41	30.30	37.60	31.00	31.31	31.16	34.94	31.27	34.07	30.08	27.41	30.50	29.14	29.09	30.54
Fe_2O_3	66.72	14.30	62.39	9.89	62.12	8.91	66.41	66.69	13.18	66.88	66.14	66.75	22.62	62.17	24.85	63.90	36.12	31.77	30.89	30.85	61.85
MnO	0.01	0.51	0.13	0.85	0.10	0.70	0.04	tr	0.74	0.004	0.004	0.002	0.37	0.08	0.49	0.05	0.14	0.08	0.13	0.14	0.17
V_2O_3	0.29	0.08	0.22	0.007	—	—	0.23	—	—	0.33	0.29	0.33	0.16	0.28	0.17	—	—	0.28	0.30	0.26	0.29
P_2O_5	—	—	—	—	0.35	0.14	—	0.48	0.16	—	—	—	—	—	—	0.77	0.62	—	—	—	—
SiO_2	0.25	0.08	0.10	0.08	0.46	0.28	0.46	0.24	0.29	0.20	0.21	0.19	0.25	0.64	0.59	0.42	0.22	0.09	0.13	0.08	0.23
MgO	0.22	0.92	0.40	1.00	0.35	0.66	0.17	tr	0.97	0.07	0.07	0.07	0.44	0.23	0.48	0.53	1.44	0.60	1.57	1.90	0.37
Al_2O_3	0.98	0.25	2.28	0.37	2.26	1.06	0.86	1.57	1.01	0.73	0.76	0.62	0.34	0.60	0.44	1.22	1.23	0.72	0.78	0.81	2.93
	99.76	100.18	99.79	100.27	99.55	99.66	99.82	100.43	99.38	100.18	99.79	100.14	100.12	100.31	100.39	99.83	99.79	[2]100.18	[3]100.09	[4]102.36	[5]99.99
$MgTiO_3$		3.4		3.7		2.2			3.3				1.3		1.1		5.2	2.3	5.8	[6]7.2	
$MnTiO_3$		1.1		1.8		1.5			1.6				0.8		1.1		0.3	0.2	0.3	0.3	
Al_2O_3		0.4		0.5		1.6			1.5				0.5		0.7		1.9	1.1	1.1	1.2	
V_2O_3		0.1		0.0		0.1			0.1				0.2		0.2		0.5	0.3	0.3	0.2	
$FeTiO_3$		82.7		88.6		88.7			82.1				76.6		73.7		57.3	66.2	64.0	61.8	
Fe_2O_3		12.3		5.4		6.0			11.4				20.6		23.3		33.7	29.9	28.5	29.3	
Fe_3O_4		0.0		0.0		0.0			0.0				0.0		0.0		1.1				
R_2SiO_4	1.1		0.4		1.8		1.8							[7]2.5		[7]0.0					
R_3O_4	2.6		5.4		5.6		2.2							[7]1.9		[7]3.6					
Fe_2TiO_4	2.7		10.8		13.3		3.5							[7]5.8		[7]6.0					
Fe_3O_4	93.4		83.4		79.5		92.5							[7]89.9		[7]90.4					
1000 MnO/FeO	0.3	13	4.3	22	3.4	18	1.3	—	20	0.13	0.13	0.06	11	[7]1.3	14	[7]1.7	5.1	2.6	4.5	4.8	
1000 V_2O_3/Fe_2O_3	4.3	5.6	3.5	0.7	[8]2.8	[8]7.9	3.5	3.5	6.1	4.9	4.4	4.9	7.1	[7]4.4	6.9	[7][8]6.0	[8]5.6	8.8	9.7	9.0	
$K(V_2O_3/Fe_2O_3)$	1.3		0.2		[8]2.8		1.7					1.4		[7]1.6		[7][8]1.4					
Ky	0.3		0.03		[8]0.4			0.3				0.5		[7]0.6		[7][8]0.8					
100 Al_2O_3/Fe_2O_3	1.5	1.7	3.7	3.8	3.6	12	1.3	2.3	7.6	1.1	1.1	0.9	1.5	[7]0.93	1.8	[7]1.9	3.4				
$K(Al_2O_3/Fe_2O_3)$	1.1		1.0		3.3			3.3				1.4		[7]1.9		[7]1.8					
K_{Al}	0.2		0.2		0.5			0.6				0.5		[7]0.7		[7]1.0					
1000 MnO/TiO_2	11	11	3.4	17	21	14	32	—	16	4	4	2	9.0	[7]20	12	[7]24	4.3				
$K(MnO/TiO_2)$	1		5		0.7			0.5		2.2				[7]0.6		[7]0.2					
K_{mn}	50		6.5		7.0			18				92		[7]12		[7]2.8					
K_{mg}	42		2.5		1.9			5.7				6.3		[7]2.3		[7]3.9					

[1] Analysis by M. Chiba, Japan Analytical Chemical Research Institute.
[2] Includes 0.11% CaO, 0.07% Cr_2O_3, 0.01% Ni.
[3] Includes 0.14% CaO, 0.10% Cr_2O_3, 0.02% Ni.
[4] Includes 0.14% CaO, 0.10% Cr_2O_3, 0.02% Ni.
[5] Includes 0.17% CaO, 0.02% Cr_2O_3, 0.01% Ni.
[6] TiO_2 assumed in error by +2.36%.
[7] Corrected for impurities, see text.
[8] Adjusted by comparison of AA252 magnetite analysed by Chiba and by Katzendorfer and Boileau, see text.

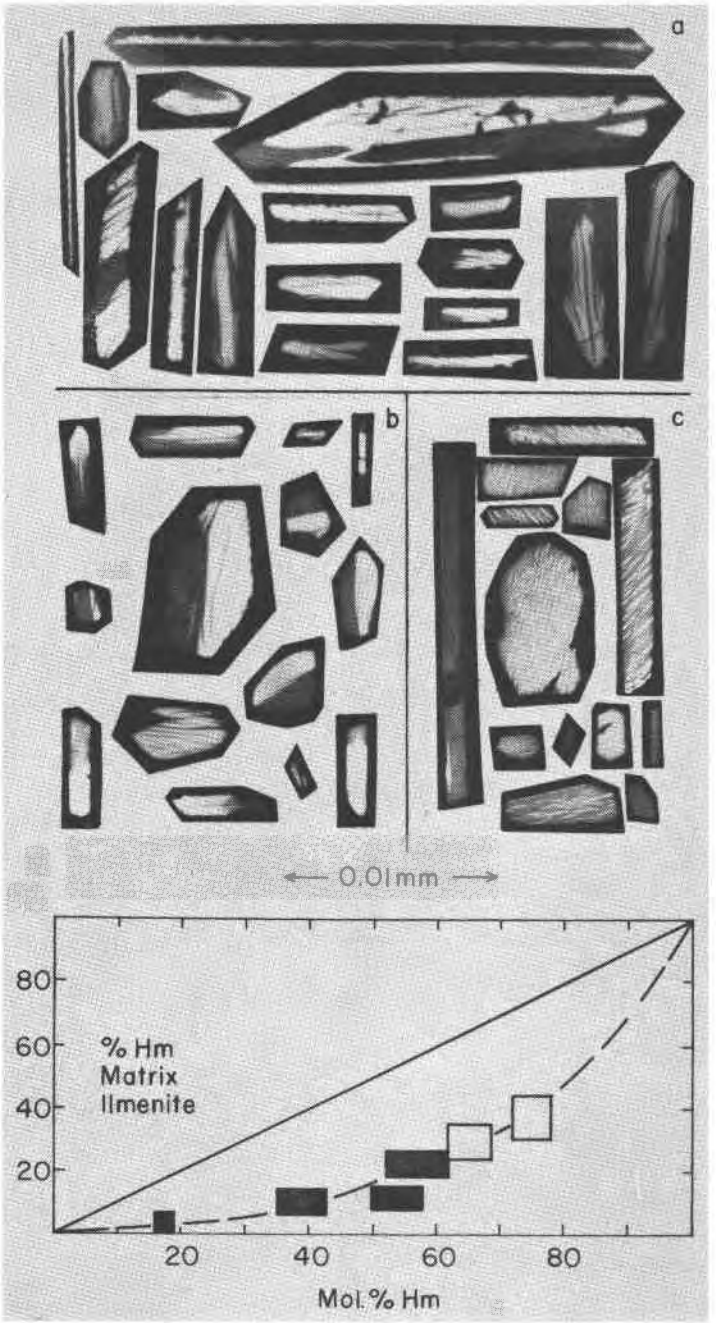

FIG. 3. Exsolution rodlets and platelets of rhombohedral oxide from feldspar. **a:** Inclusions in antiperthite megacryst, A591 (estimated average composition = Hm 75). **b:** Inclusions in antiperthite megacryst A92 (analysed average composition = Hm 53). **c:** Inclusions in zoned plagioclase—antiperthite megacryst A128 (analysed average composition = Hm 17). **d:** The composition of oxide inclusions exsolved from feldspar (horizontal axis) plotted against that of co-existing matrix (hemo-) ilmenite (vertical axis).

oxide-rich gabbro in the Sault-aux-Cochon complex. Three of the analyzed biotites are deficient in water plus fluorine and are therefore oxybiotites. The biotite from A128 oxide-rich gabbro is low in potassium and high in water, suggesting hydronium substitution for potassium.

TABLE 6. PYROXENE ANALYSES

	Clinopyroxenes						
	A9b	A128	A168	AA252	A408	A569	A604
Ca	15.3	14.6	14.3	14.5	16.3		15.6
Mg	6.7	6.7	4.9	6.2	7.1		6.5
Fe	9.4	9.6	13.8	10.5	8.0		9.4
Mn	0.24	0.33	0.33	0.30	0.23		0.25
Al	1.27	1.34	0.81	1.01	1.42		1.22
Ti	0.11	0.16	0.12	0.12	0.17		0.16
Mol.: Mg/Mg+Fe	0.62	0.62	0.45	0.58	0.67		0.61
	Orthopyroxenes						
	A9b	A128	A168	AA252	A408	A569	A604
Ca	0.38	0.45	0.60	0.42	0.41	0.36	0.41
Mg	10.4	10.5	6.6	9.4	11.5	13.3	10.7
Fe	21.7	21.8	28.1	24.6	20.7	18.1	21.6
Mn	0.54	0.70	0.76	0.76	0.51	0.27	0.59
Al	0.56	0.70	0.38	0.52	0.76	0.89	0.69
Ti	0.07	0.08	0.08	0.07	0.09	0.08	0.09
γ	1.723	1.719	1.735	1.724	1.715	1.709	1.720
EN[1]	53	57	43	52	60	65	55
Mol.: Mg/Mg+Fe	0.52	0.52	0.35	0.47	0.56	0.63	0.53
Wt.: Mg/Mg+Fe	0.32	0.32	0.19	0.28	0.36	0.42	0.33
Wt.: Mn/Fe	0.025	0.032	0.027	0.031	0.025	0.015	0.027
Mol.: $\frac{(Mg/Mg+Fe)OPX}{(Mg/Mg+Fe)CPX}$	0.84	0.85	0.78	0.81	0.84		0.87

[1] Mol percent enstatite deduced from the curves of Hess (1960).

Biotites from gabbroic anorthosite and oxide-rich gabbro in the Sault-aux-Cochon complex are slightly richer in lithium than are those in the border facies oxide-rich gabbro and core facies noritic anorthosite.

(*f*) Oxygen isotope analyses. The results of the oxygen isotope analyses of the feldspars, apatites and iron-titanium oxide minerals are reproduced in Table 9. There is a conspicuous correlation between the oxygen isotopic compositions of the minerals and the modal abundances of iron-titanium oxide minerals in the rock samples which are plotted in Fig. 5.

Discussion

Recrystallization. In order to interpret the chemical and mineralogic attributes of the Labrieville massif in terms of any primary processes, the effects of recrystallization must be understood. The following summarized

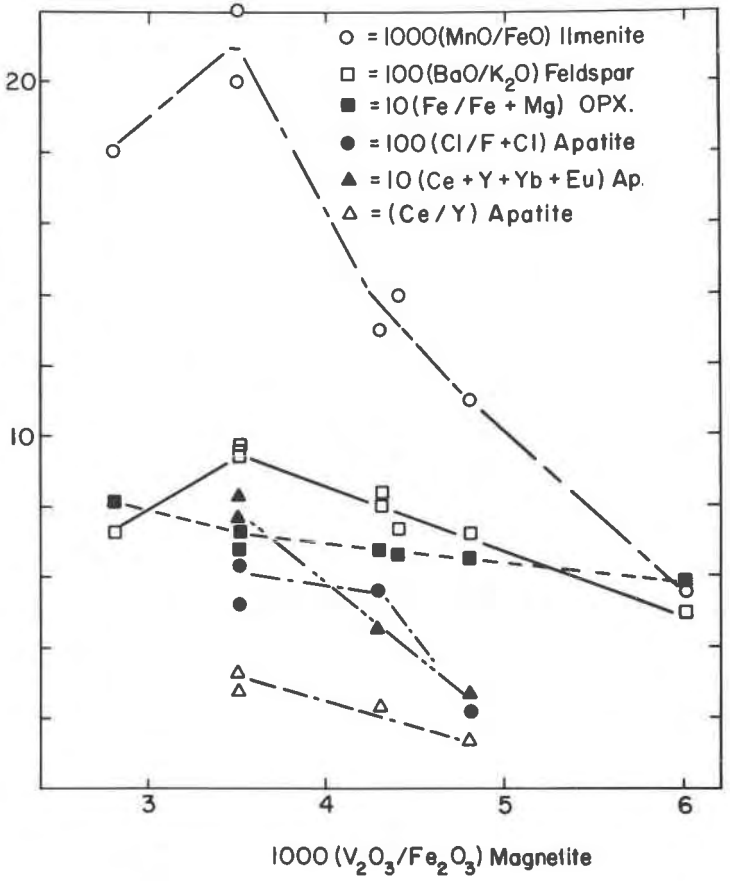

Fig. 4. Various parameters of crystallization differentiation and the V_2O_3/Fe_2O_3 ratio of magnetite.

observations indicate that recrystallization of the Labrieville rocks, whereas profound on a scale of a few millimeters, has had no detectable effect over dimensions much greater than a few centimeters.

The 3-mm wide rim of zoned plagioclase surrounding the labradorite anorthosite xenolith demonstrates that extensive homogenization of the feldspars is out of the question. Likewise the zoning of mesoperthite-

TABLE 7. APATITE ANALYSES

	A9b	A128a	A128b[1]	A408	A408II	B11–92	B11–131.5
P_2O_5	40.81	39.92	39.92	41.39	40.85		41.59
CaO	54.82	54.1	54.23	54.68	53.69		53.14
MgO	0.08	0.10	0.11	0.11			
MnO	0.04	0.07	0.04	0.02			
FeO	0.00	0.06	0.06	0.06	0.19		0.53
Fe_2O_3	0.17	0.00	0.10	0.00	0.24		0.40
Na_2O	0.05	0.07	0.07	0.05			
K_2O	0.01	0.01	0.01	0.01			
Li_2O	0.00	0.00	0.00	0.00			
Al_2O_3	0.10	0.06	0.16	0.06			
TiO_2	0.02	0.02	0.02	0.008			
SiO_2	0.53	0.51	0.57	0.01	0.30		0.11
F	3.00	3.10	3.38	3.38	3.66	3.55	3.52
Cl	0.18	0.21	0.20	0.08	0.12	0.10	0.09
H_2O total	0.23	0.18	0.13	0.15	0.39	0.45	0.37
CO_2	0.00	n.d.	0.03	0.06			
Sr	0.10	0.15	0.16	0.08			
Ba	0.001	0.001	0.001	0.001			
Ce	0.31	0.60	0.58	0.16	0.07	0.06	0.04
Eu	0.001	0.005	0.005	0.001	0.002	0.002	0.002
Y	0.15	0.21	0.18	0.10	0.09	0.04	0.04
Yb	0.006	0.007	0.007	0.003	0.004	0.002	0.002
Σ	100.61	99.38	99.96	100.41	99.60		99.83
less O for F, Cl	1.30	1.35	1.47	1.44	1.57		1.50
Σ[1]	99.31	98.03	98.49	98.97	98.03		98.33
Cl/F+Cl	0.057	0.063	0.056	0.023	0.032	0.028	0.025
Eu/Yb	0.2	0.7	0.7	0.3	0.5	1.0	1.0
Ce/Y	2.1	2.9	3.2	1.6	0.8	1.5	1.0
Y+Ce+Yb+Eu	0.47	0.82	0.77	0.26	0.17	0.10	0.08

[1] Not treated with 6:1 HNO_3.

mantled plagioclase megacrysts in syenite is developed over a small dimension of a few millimeters. The greater Or content of the plagioclase phase of antiperthite and plagioclase megacrysts compared to that of matrix plagioclase and antiperthite indicates that equilibrium was limited to a few millimeters during subsolvus cooling.

The difference between the chemical composition of opaque rodlets in feldspar megacrysts and the composition of large grains of (hemo-) ilmenite in the matrix of the rocks indicates that oxygen fugacity gradients existed over dimensions of several millimeters during the early

(pre-hematite-ilmenite exsolution) cooling history. Similarly, the relict zoning of hemo-ilmenites adjacent to magnetite indicates the extremely local influence of oxidation-reduction agents.

The systematically variable compositions of individual minerals con-

TABLE 8. BIOTITE ANALYSES

	A569	A408	A9b	A128
SiO_2	37.89	38.37	37.71	35.78
Al_2O_3	14.03	12.92	13.52	13.39
Fe_2O_3	1.27	1.15	1.53	7.35
FeO	11.38	12.42	13.55	7.56
CaO	0.28	0.34	0.06	0.34
MgO	17.00	17.29	14.53	13.59
TiO_2	5.24	5.03	5.55	6.29
Na_2O	0.25	0.20	0.13	0.19
K_2O	9.70	9.21	8.97	6.54
Li_2O	0.005	0.006	0.007	0.007
MnO	0.009	0.014	0.019	0.014
H_2O	1.72	1.86	3.46	7.93
F	0.60	0.95	0.33	0.53
Total	99.37	99.76	99.37	99.51
2-(OH+F)	0.98	0.26	0.19	0.0
I(004)/I(005)	0.734	0.54	0.61	0.64
β	1.633	1.632		1.642
$\mu \times 10^{-6}$		22	25	23

I(004)/I(005) = ratio of intensity of x-ray diffraction peaks measured by weighing cut-outs of diffractometer tracings. Samples were prepared by precipitating finely ground biotite onto glass disks which were dried and x-rayed using a spinner attachment.

β = the refractive index of biotite flakes lying on a cleavage surface.

$\mu \times 10^{-6}$ = the mass magnetic susceptibility determined according to the method of Hess in his notes on the operation of the Frantz Isodynamic Magnetic separator.

2 − (OH+F) = the "oxy content" of the biotites calculated according to a unit biotite formula of the form: $K(Mg, Fe, Ti)_{3-x}(Al, Fe, Ti)(Si, Al)_3O_{10}(OH, F, O)_2$.

clusively prohibit equilibrium communication between rocks during any part of their crystallization and cooling history, since it is quantitatively impossible to account for the compositional variations on the basis of infra-rock redistribution of chemical components between the observed minerals during recrystallization.

The correlation between the oxygen isotopic compositions of the several minerals and the modal abundance of iron-titanium oxide minerals

in the rocks indicates not only that redistribution of oxygen isotopes did take place between coexisting minerals, but also that this redistribution was limited to the local (modally unique) environment.

Crystallization and Differentiation (*a*) Oxygen isotope measurements. The oxygen isotopic fractionation between coexisting (hemo-) ilmenite and plagioclase is larger (about 4.5 per mil) than that observed between the same minerals from the Skaergaard intrusion (about 3.3 per mil, Taylor

TABLE 9. OXYGEN ISOTOPE ANALYSES

	Bulk Feldspar	Feldspar Megacrysts	Apatite	Ilmenite	Magnetite	Ilmenite Lamellae in Magnetite
A9b	7.4	7.1		2.4	0.9	
A117		7.0				
A128	8.0	7.6	7.2	3.0	1.8	3.0
A168	7.7			2.1	−0.2	
AA241	7.4					
AA252	7.9			2.8	1.4	
AA242 host	7.3					
AA242 xenolith	7.0					
A408	8.4	8.0		3.3	2.2	
A569	7.2			2.2	1.0	
A591		7.0				
A604	7.5			2.0	1.0	
B11-92			8.0	4.1		
B11-166.5				4.8		
B13-77-80				4.9		

All numbers are per mil deviations from the SMOW standard of Craig (1961).

and Epstein, 1963) and suggests relatively lower temperatures of recrystallization. However, there is a convincing correlation between the oxygen isotopic composition of the (hemo-) ilmenites and the modal abundance of ion-titanium oxide minerals in the rocks, Fig. 5. This correlation is independent of the differentiation sequence and cannot be due to crystallization differentiation of oxygen isotopes. The correlation is a natural consequence of closed system, retrograde recrystallization: as temperature decreases the fractionation of oxygen isotopes between oxides and silicates increases, and material balance within a locally closed system requires that the resultant oxygen isotopic composition of all minerals participating in the retrograde recrystallization reflects the modal composition of the rock. Accordingly all minerals in a rock initially rich in

iron-titanium oxide minerals will acquire an O^{18}-rich composition as a result of retrograde recrystallization relative to those in a rock initially rich in feldspar. The (hemo-) ilmenite in an ilmenite rock will retain the primary oxygen isotopic composition of the ilmenite, and the feldspar in a feldspar rock will retain its primary isotopic ratio; therefore, the primary plagioclase-ilmemite oxygen isotopic fractionation may be

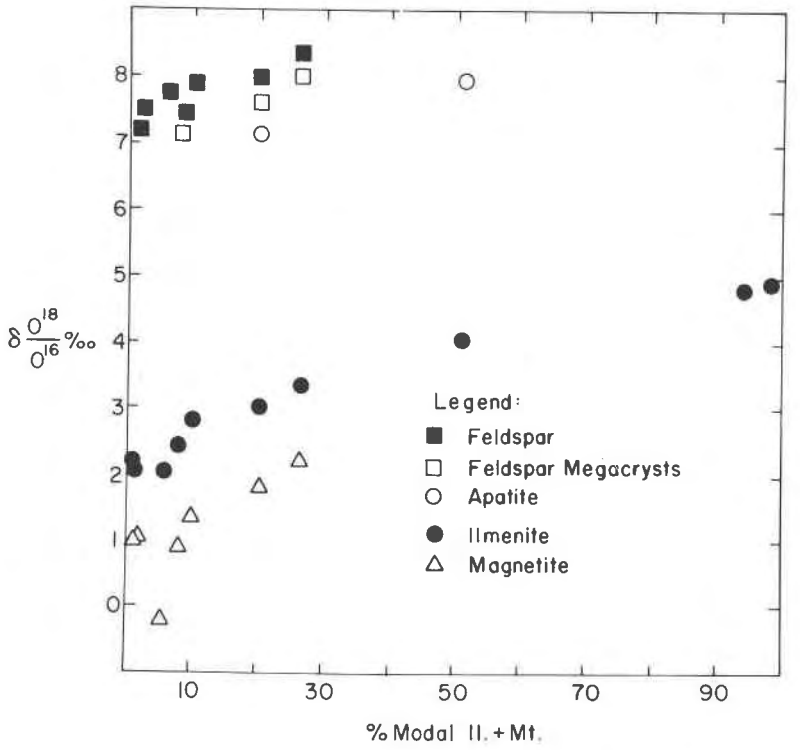

FIG. 5. The oxygen isotopic composition of various minerals and the modal abundance of iron-titanium oxide minerals.

deduced. From Fig. 5, it is about 2.0 per mil, or 1.3 per ml smaller than that observed in the Skaergaard intrusion.[1] At high temperatures, the magnetite-ilmenite fractionation is less than 0.5 per mil (Anderson, in preparation), indicating that a primary plagioclase-magnetite fractionation for the Labrieville anorthosite would be less than 2.5 per mil, which is precisely the plagioclase-magnetite fractionation deter-

[1] Compositions of coexisting magnetite and ilmenite in the Skaergaard intrusion suggest relatively low temperatures of (re) crystallization (about 900°C, Vincent and Phillips, 1954; Buddington and Lindsley, 1963).

mined for a basalt (Anderson and Clayton, 1966). It seems safe to conclude that the primary separation of ilmenite from plagioclase in the Labrieville anorthosite occurred at very high temperatures, as high or higher than those characteristic of the crystallization of magnetite and plagioclase in basalt (probably about 1100° C).

(*b*) Feldspars. The Labrieville antiperthites, like other antiperthites (Sen, 1961), are compositionally similar to the potassic plagioclases of rhomb porphyrites and of mugearites and hawaiites (Muir and Tilley,

TABLE 10. FELDSPAR COMPOSITIONS

	Mol % An	Mol % Or	Mol % Cn	Wt % SrO	Wt % Fe	Wt % TiO_2	Wt % BaO	BaO Wt——×100 K_2O	Locality	Ref.[1]
Anorthosite	48.1	3.6		0.18	0.16	0.04	0.02	3.5	Adirondack, N. Y.	1
Rectangle Porphyry	44.7	7.8		0.16	0.37		0.13	9.5	Oslo graben, Norway	2
Charnockite	37.7	6.3							Madras, India	3
Ferro Gabbro	41.0	2.7		0.41	0.50	0.00			Skaergaard, Greenland	4
Granodiorite	37.2	1.9		0.08	0.03	0.02	0.03	9.4	Crestmore, Calif.	1
Andesite	35.4	4.4		0.33	0.30		0.097		Germany	2
Alkali Basalt	41.9	5.8		0.30	0.41		0.092		Germany	2
Hawaiite (4)	33.3	11.8							Mauna Kea, Hawaii	5
Mugearite (17)	26.7	11.1							Puukawaiwai, Hawaii	5
Trachyte (6B)	37.5	6.7							Tristan da Cunha	6
Rhomb Porphyry	34.7	11.5		0.36	0.38	0.14	0.16	8.1	Oslo graben, Norway	2
Anorthosite (9b)	36.1	8.0		0.39	0.22	0.08	0.11	8.3	Labrieville, Que.	7
Pitchstone (12B)	15.5	7.8							Antrim, U. K.	8
Mugearite (17)	15.6	20.6							Mauna Kea, Hawaii	5
Hawaiite (4)	11.6	27.9							Puukawaiwai, Hawaii	5
Trachyte (6A)	2.4	50.2							Tristan da Cunha	6
Pitchstone (12A)	2.2	66.1							Antrim, U. K.	8
Syeno-gabbro	21	38		0.25	0.1				Labrieville, Que.	7
Syenite	17	31	0.7					7.2	Labrieville, Que.	7

[1] References: 1 Emmons (1953); 2 Sen (1959 and 1960); 3 Howie (1955); 4 Wager and Mitchell (1951); 5 Muir and Tilley (1961); 6 Carmichael (1963 and 1965); 7 this paper.

1961). Andesines in granodiorites, quartz monzonites and granites and their volcanic equivalents are generally much less potassic (Sen, 1961; Carmichael, 1960). Some typical feldspar compositions are listed in Table 10 for comparison. Sen (1961) concluded that the relatively high potassium contents of antiperthites most probably result from high temperatures of crystallization with bulk liquid composition playing a secondary role.

The normative plagioclase in the mugearite and hawaiite described by Muir and Tilley (1961) is only a few per cent poorer in An than the corresponding plagioclase. Likewise, the deduced normative plagioclase of the Skaergaard residual liquid was only slightly more sodic than the crystals in the andesine range (Wager, 1960). In contrast, the Ab/An crystal liquid fractionation in the pure plagioclase system is about 30 per cent

at a crystal composition of An 35 (Bowen, 1913). Therefore, it is likely that the relatively constant An/(Ab+An) ratio of plagioclase and antiperthite in the Labrieville massif is a result of a relatively small crystal-liquid fractionation of An relative to Ab.

The mesoperthites in the syeno-gabbro (AA252) and syenites(A168 and A117) are compositionally similar to the anorthoclase found in larvikite (Muir and Smith, 1956) and mugearite and hawaiite (Muir and Tilley, 1961).

Yoder, Stewart and Smith (1957) pointed out that the slope of the feldspar tie lines in the Ab, An, Or system is a fair indicator of water

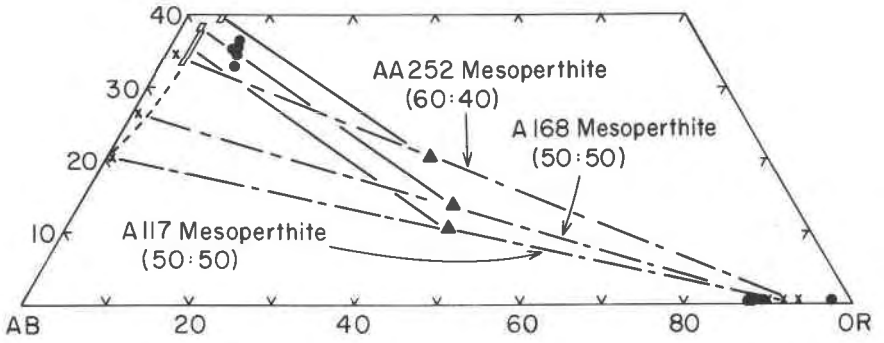

FIG. 6. Labrieville feldspar compositions. (The proportions of plagioclase and potassium feldspar in the mesoperthites were determined by point count analysis of polished single crystals at 2400× magnification.)

pressure (or temperature) of crystallization. The coexisting feldspars in the mesoperthite and plagioclase bearing rocks of the Labrieville massif have tie lines suggesting relatively low water pressures (or high temperatures) of crystallization.

The analyzed feldspars of the Labrieville massif are plotted on Fig. 6. Judging from the location of the feldspar tie lines from the syenite, A168, and the syeno-gabbro, AA252, the liquid from which these feldspars crystallized had a composition which would plot to the Ab side of the tie lines. Using the bulk feldspar analyses of these two nearly mono-feldspathic rocks as a rough guide, the more highly differentiated syenite liquid was richer in Or than the syeno-gabbro parent liquid.

A diagrammatic pseudo-binary projection of the presumed course of feldspar crystallization in qualitative terms is given in Fig. 7.

The positive correlation between An and Or content of the plagioclase phase of mesoperthite-mantled plagioclase megacrysts in syenite suggests that the Al/Si ratio of the feldspar controlled the extent of exsolution of

orthoclase: the higher the Al/Si ratio of the primary feldspar, the more difficult and sluggish the exsolution of orthoclase.

Both the orthoclase occurring in antiperthite and that occurring in mesoperthite is much poorer in Fe than the plagioclase phase. There is a crude positive correlation between the ratio: Fe(plagioclase)Fe/(orthoclase) and the An content of the plagioclase, suggesting that the distribution of iron between plagioclase and orthoclase is compositionally controlled: the more aluminous the plagioclase, the more the available substitutional sites for iron, thus more iron.

Similarly the distribution of strontium between plagioclase and ortho-

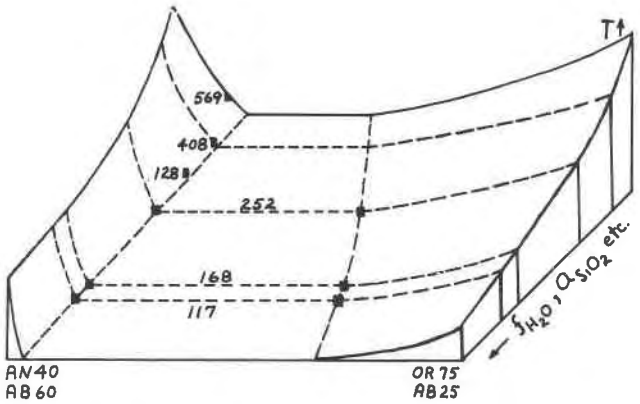

FIG. 7. The crystallization trend of Labrieville feldspars, schematic.

clase reflects the An content of the plagioclase: the more the substitutional (Ca) sites in the plagioclase, the higher is the ratio: Sr(plagioclase)/Sr(orthoclase).

The BaO/K_2O ratio of the Labrieville feldspars changes by a factor of two throughout the lithologic sequence. Whether this is to be regarded as a large or small change depends upon the fractionation factor relating the BaO/K_2O ratio in the feldspar crystals and the liquid from which they crystallized. Values of (BaO/K_2O)feldspar/(BaO/K_2O) liquid (hereafter called R1) are listed below:

Or	*An*	*R1*	*Reference*
2.8	55.7	0.98	Walker, Vincent and Mitchell, 1952
2	54	0.55	Wager and Mitchell, 1951 (B, table 6, p. 154)
3	40	1.1	Wager and Mitchell, 1951 (D, table 6, p. 154)
2	37	2.8	Wager and Mitchell, 1951 (E, table 6, p. 154)
5	17	2.67	Carmichael and McDonald, 1961 (8F and 12G)
12	11	>3.75	Carmichael and McDonald, 1961 (7F and 3G)

An obvious correlation exists between An and R1. Although interpolation of this data ignoring data points at An 37 and An 11 suggests an Rl value slightly greater than 1 for the Labrieville antiperthites, it is concluded that Rl was, in fact, less than 1, since an increase in BaO/K_2O is observed. Assuming Rl equal to 0.5 as a lower limit, the Rayleigh distillation equation shows that an increase in BaO/K_2O by a factor of 2 requires that at least 75 per cent of the feldspar components present in the liquid when the rock A569 crystallized must have crystallized by the stage of crystallization of oxide-rich gabbro A128. In these terms the observed two-fold increase in BaO/K_2O in the antiperthites is large and requires a great deal of fractional crystallization of feldspar constituents with a

TABLE 11. FRACTIONATION STAGES

	A569	A408	A604	A9b	A128	A252	A168	Basis
f(PL)	100	50	54	39	26	38		$(BaO/K_2O)XL/(BaO/K_2O)LIQ = 0.5$
f(PL)*	100	7	10	3	.6	.8		$(BaO/K_2O)XL/(BaO/K_2O)LIQ = 0.87$
f(PX)	100	56	44	40	41	24	7	$(MgO/MgO+FeO)XL/(MgO/MgO+FeO)LIQ = 1.39$
f(OX)	100	74	62	61	44	44	16	$(V_2O_3/Fe_2O_3)XL/(V_2O_3/Fe_2O_3)LIQ = 1.67$

$f = \left(\frac{R_{A569}}{R_f}\right) \exp \left(\frac{1}{1-\alpha}\right)$ where $\alpha = \frac{R_{crystals}}{R_{liquid}}$, assumed constant during crystallization, and where R may be any of the listed ratios.

f(PL, PX, OX) = fraction of plagioclase, pyroxene or oxide constituents remaining in the liquid at each rock stage relative to A569.

less than 25 per cent approach to equilibrium crystallization. Fractionation stages for the various rocks calculated according to the above assumptions are given in column 1 of Table 11.

The BaO/K_2O ratio of the mesoperthite in A168 syenite is smaller than it is in oxide-rich gabbro and mesoperthite gabbro. This is expected in view of the probably large value (>1) of the Rl fractionation factor between an alkali feldspar and liquid, which would cause the residual liquids to become depleted in barium relative to potassium.

Papezik (1965) reports increasing Ba/K ratios in the progressive differentiation sequence: anorthosite, gabbroic anorthosite, oxide-rich gabbro (called ferrogabbro by him) of the Morin anorthosite which has plagioclase mostly near An 48. The Ba/K ratios found by Papezik increase by a factor of 4. The smaller increase by a factor of 2 in the Labrieville anorthosite can easily be explained on the basis of a primary fractionation factor (Rl) closer to 1 due to its more sodic plagioclase. Papezik pointed out that the Ba/K ratios correlate positively with the Co/Ni ratio and negatively with the cr/Fe^{3+} ratio of the rocks.

Although a ratio of Rl = 0.5 was assumed to calculate the *minimum*

amount of feldspar crystallization, this value is unreasonably small in view of Papezik's (1965) data on the Morin anorthosite, suggesting it to be at least 94 per cent perfectly fractionated at the ferrogabbro stage if the same Rl=0.5 is assumed. If Rl is assumed to be 0.7 for the Morin anorthosite (a better assumption in the light of published data; see above), then the Rl factor for the Labrieville anorthosite would be 0.87 to achieve the same degree of fractionation at the ferrogabro or oxide-rich gabbro stage. According to these fractionation factors, the original BaO/K_2O ratio for the Labrieville liquid would have been 0.059 and for the Morin liquid 0.050 compared to 0.046 for Antarctic mugearite, 0.042 for hawaiite and about 0.034 for tholeiite and alkali olivine basalt (Gunn, 1965). If the Labrieville anorthosite came from a source similar to that of basaltic rocks, then it is either a highly fractionated residuum (less than 30 per cent of the original liquid) or a product of less complete partial fusion.

The average compositions of rodlets and platelets of rhombohedral oxide occurring in feldspar megacrysts in core and border facies anorthosite and gabbroic anorthosite is approximately 70 per cent hematite (Fig. 3).[1] Later rock types have megacrysts whose hemo-ilmenite inclusions are poorer in hematite and decrease to about 15 per cent in syenite. In all cases, there is a higher proportion of hematite in the opaque rodlets exsolved from feldspar megacrysts than there is in coexisting matrix (hemo-) ilmenite. Since the titanium remaining in solid solution in the feldspar is trivial (Table 3) and since the iron in the feldspar lattice is constant within about 10 per cent of the amount present (Table 3), it is concluded that the compositional difference between the opaque rodlets and the matrix (hemo-) ilmenite is due to exsolution of iron and titanium oxides from a ferri-titano-ferrous plagioclase ancestor and that the rodlets derived their compositions from the ferrous and ferric iron and titanium ratios of the plagioclase ancestor.

Several megacrysts contain exsolved opaque rodlets with an average composition near the crest of the hematite-ilmenite solvus. Carmichael's (1961) determination indicates that the crest lies at about 950° C. Even allowing for an undercooling of 100° C., the compositions of the hemo-ilmenite and ilmeno-hematite rodlets require exsolution from their plagioclase host at temperatures above 850° C., a conclusion which is in agreement with Sen's (1960) data indicating that only at quite high temperatures is as much as a few tenths of a per cent of iron and titanium accepted into the plagioclase lattice.

[1] Although the opaque inclusions occurring in silicates usually are not positively identified, as early as 1936 Newhouse identified the opaque inclusions in anorthosite feldspars, and his published photograph (Plate 12, Fig. 2) clearly reveals their highly hematitic nature.

(*c*) Structural state measurements. The plagioclase phase of the Labrieville feldspars has a low structural state indicative of slow cooling.

Although the plagioclase phase has a low structural state, the potassium feldspar in antiperthite has the properties of orthoclase (Goldsmith and Laves, 1954) rather than microcline. The cause of this is unknown.

(*d*) Iron-titanium oxide minerals. With two exceptions, the compositions of coexisting ilmeno-magnetites and (hemo-) ilmenites cannot be used to deduce actual temperatures and oxygen fugacities of equilibration because the compositions plot in the highly oxidizing, uninvestigated part of Lindsley's diagram (Buddington and Lindsley, 1964). The two exceptions are the Sault-aux-Cochon oxide-rich gabbro, A128 (about 620° C., $10^{-19.5}$ atm f_{O_2}), and syenite, A168 (640° C., $10^{-18.8}$ atm f_{O_2}).

The Fe_2O_3 content of matrix (hemo-) ilmenite decreases progressively from about Hm 34 in core facies anorthosites and noritic anorthosite to about Hm 6 in Sault-aux-Cochon oxide-rich gabbro and syenite. Several factors may contribute to the composition of (hemo-) ilmenite in any particular rock:

(1) granule exsolution of relatively ferric iron-rich hemo-ilmenite or ilmeno-hematite from feldspar;
(2) granule exsolution of relatively Hm poor ilmenite from ilmeno-magnetite;
(3) loss of ferric iron in primary (hemo-) ilmenite consumed by the oxidation of ulvospinel in (magnetite+ulvospinel) solid solution according to the reaction: $Fe_2O_3 + Fe_2TiO_4 = Fe_3O_4 + FeTiO_3$;
(4) reduction of primary ilmenite by water during cooling.

Since most of the rocks studied contain more than several times as much (hemo-) ilmenite as could be derived by means of granule exsolution of feldspar (Table 1), the quantitative effect of such a process is generally negligible. However, most of the core facies rocks contain less than about 1 per cent rhombohedral oxide. Areal analysis of polished slabs of A569 and A591 revealed only 0.5 ± 0.1 and 0.8 ± 0.1 per cent hemo-ilmenite respectively, relative to 100 per cent feldspars. If the feldspar in A569 initially contained 0.2 per cent of iron-titanium oxide of the likely composition of Hm 75, complete exsolution would contribute 0.15 per cent hematite to the matrix hemo-ilmenite. The amount of hematite in matrix hemo-ilmenite in A569 is 0.17 per cent. Obviously such a process might account for the present Hm-rich composition of the matrix hemo-ilmenite in the core facies. However, if the major part of the matrix hemo-ilmenite were derived ultimately from feldspar, then the composition difference between exsolution rodlets and matrix hemo-ilmenite would be greatly diminished in rocks poor in matrix hemo-ilmenite. In fact, the composition difference is just as great in AA241 and A591 as it is in A408 (there are no megacrysts in A569). The solution to this paradox appears to lie in the two sorts of matrix rhombohedral oxide evident in

core facies rocks: one sort occurs as relatively large masses (more than a few square millimeters on polished surface) associated with pyroxene, biotite and apatite. These larger masses have a composition near Hm 30. In addition there are appreciable quantities of intergranular rhombohedral oxides which cover relatively small areas (less than one square millimeter) in many of which the predominant phase is hematite and the bulk composition is near Hm 70. It appears likely that the separation procedure used to obtain a rhombohedral oxide separate from A569 selectively concentrated hemo-ilmenite from the large masses of rhombohedral oxide in the rock. Therefore, it is concluded that the analysed composition of A569 hemo-ilmenite fairly adequately reflects the composition of the primary rhombohedral oxide in that rock and that occurrences of intergranular ilmeno-hematite represent recrystallized rhombohedral oxide exsolved from feldspar.

In rocks such as the oxide-rich gabbro, A128, and syenite, A168, in which ilmeno-magnetite is the predominant iron-titanium oxide mineral, the possibility exists that significant amounts of ilmenite have been added to the matrix (hemo-) ilmenite by external granule "exsolution" of ilmenite from magnetite (see Buddington and Lindsley, 1964). If cooling occurs under dry, closed system conditions, then the primary ferrian ilmenite and titaniferous magnetite will react according to the equation $Fe_2O_3+Fe_2TiO_4=Fe_3O_4+FeTiO_3$ because of the opposing trends of the two isocompositional cooling curves in terms of oxygen fugacity (Fig. 8). On the other hand, the cooling of water at constant H_2/H_2O ratio (or constant bulk composition), although slightly reducing relative to the isocompositional cooling of ilmenite, is strongly oxidizing relative to the isocompositional cooling of titaniferous magnetite. Buddington and Lindsley (1964) point out that although a small proportion of water to titaniferous magnetite suffices to oxidize ulvospinel to ilmenite and magnetite, a much higher proportion of water to ferrian ilmenite is required to accomplish any reduction of ilmenite during closed system cooling of a rock. In a rock containing both primary titaniferous magnetite and ferrian ilmenite together with a small proportion of water, the composition of the primary ilmenite will largely govern the oxygen fugacity of the environment during cooling, the water serving to supply the oxygen needed to oxidize the ulvospinel. Therefore, in contrast to dry, closed system cooling, cooling in the presence of water and ferrian ilmenite in a closed system will produce "exsolved" ilmenite (from oxidation of titaniferous magnetite) identical in composition to that already present in the rock, and there will be no net effect on the resultant composition of the final (hemo-) ilmenite.

Apparently the proportion of titaniferous magnetite to water will

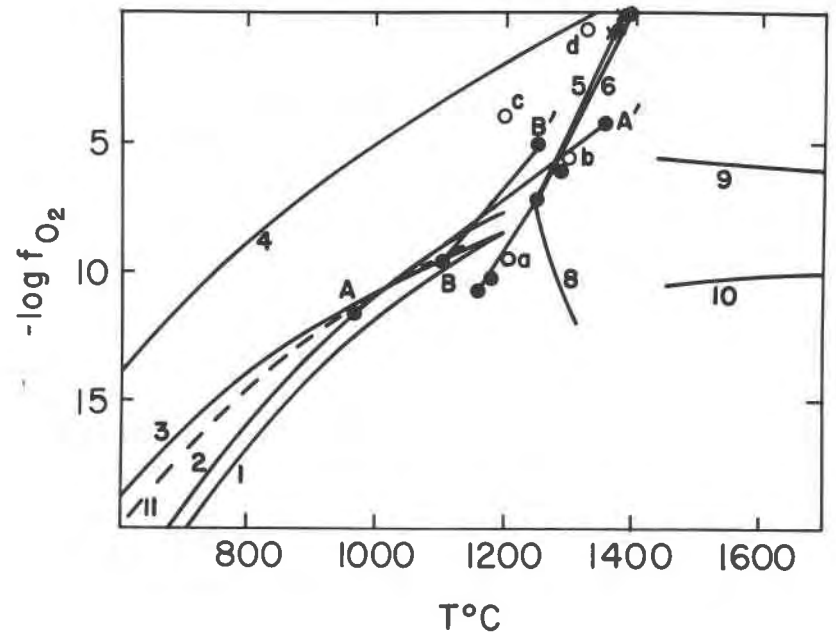

FIG. 8. The oxygen fugacity—temperature crystallization trend of the Labrieville massif compared to various univariant curves. Curves 1–4 are copied from Buddington and Lindsley (1964), curves 5–8 calculated from the data of Muan and Osborn (1956), curves 9 and 10 from Wriedt and Chipman (1956), curve 11 was taken from the tabulation of Wagman *et al.* (1945). The points labeled a–d correspond to the following compositions: a (Hm 12), b (Hm 37), c (Hm 45), d (Hm 80) and were obtained from the data of Webster and Bright (1961) at 1200° C and Taylor (1964) at 1300° C. The lines A′–A and B′–B are possible crystallization paths for the Labrieville massif. The curves are: 1) Usp 80, 2) Usp 60, 3) Hm 10, 4) Hm 100+Mt 100, 5) tridymite+pyroxene+magnesioferrite+liquid, 6) olivine+pyroxene+magnesioferrite+liquid, 7) tridymite+olivine+magnesioferrite +liquid, 8) olivine+pyroxene+tridymite+liquid, 9) Ni melt containing 0.2% oxygen, 10) Fe melt containing 0.2% oxygen, 11) $H_2O+H_2+O_2$, H_2/H_2O constant.

determine how much reduction of ferrian ilmenite takes place during subsolidus cooling of ferrian ilmenite plus titaniferous magnetite assemblages. The selective zoning of hemo-ilmenites adjacent to ilmeno-magnetite suggests that the ferrian ilmenites served as oxidizing agents, at least during the final stages of oxidation of the titaniferous magnetites.[1] Likewise, the absence of magnetite associated with the ilmeno-

[1] The compositions of the ilmeno-magnetites suggest, in the light of Lindsley's experiments (Buddington and Lindsley, 1964), that the zoning of hemo-ilmenite adjacent to magnetite developed either below about 600° C. or in association with magnetites which contained considerably higher proportions of ulvospinel in solid-solution than is now indicated by the existing ilmenite lamellae in the coexisting ilmeno-magnetites.

hematite and hemo-ilmenite rodlets exsolved from antiperthite and plagioclase megacrysts suggest local rather than general control of oxidation and reduction during cooling. Since reduction and oxidation seem to have been so locally controlled, it is likely that the ilmenite in the magnetite-rich rocks AA252, A128 and A168 has been somewhat reduced. However, the extent of reduction can hardly have been very significant because the compositions of hemo-ilmenite rodlets exsolved from plagioclase megacrysts in these rocks suggest, by analogy with the other rocks, that the magnetite-rich rocks contained a relatively Fe_2O_3-poor ferrian ilmenite to begin with. (It was argued in (a) above that the abundance and compositions of the rodlets exsolved from feldspar megacrysts indicate exsolution temperatures of 850° C. or greater—temperatures much higher than the completion of oxidation of the titaniferous magnetites.)

Conceivably, water in excess might reduce some Fe_2O_3 in ilmenite to Fe_3O_4 during cooling. It seems likely that the rare magnetite lamellae in hemo-ilmenite have developed by reduction because they are not accompanied by comparable amounts of rutile. Perhaps in the massive ilmenite rocks where magnetite is almost absent, some magnetite lamellae may have resulted from reduction by water.

All things considered, it is concluded that the presently observed compositions of the (hemo-) ilmenites closely approximate those which originally crystallized.

In view of the change in composition of the (hemo-) ilmenites from Hm 34 to Hm 6 during differentiation, it may be concluded from Fig. 8 that progressive crystallization differentiation of the Labrieville massif led to a reducing residuum relative not only to the cooling curves of isocompositional ferrian ilmenites, but also to that of water and even to those of isocompositional titaniferous magnetites, if a crystallization interval of 400° C. or less is assumed. As will be shown below, the crystallization of the Labrieville massif may be limited within the limits of about 1380° C. and 880° C., in which case the differentiation would have followed approximately the line A—A′ on Fig. 8. If the more normal crystallization interval of 1250° to 1050° C. applied, then the line B—B′ would have been followed. Line B—B′ is very nearly parallel to those of the ferrite-bearing, univariant, crystal+liquid assemblages studied by Muan and Osborn (1956).

Goldschmidt (1954) and Wager and Mitchell (1951), among others, have shown that the vanadium content of magnetite decreases during crystallization differentiation. The V_2O_3/Fe_2O_3 ratio of the Labrieville ilmeno-magnetites correlates with the BaO/K_2O ratio of the feldspars

as shown in Fig. 4. This correlation implies that crystallization of iron and titanium oxide minerals accompanied the crystallization of feldspar during consolidation of the Labrieville massif.

The stages of fractionation of iron-titanium oxide components were calculated according to the Rayleigh distillation equation using a fractionation factor of $0.60 = (V_2O_3/Fe_2O_3)$liquid$/(V_2O_3/Fe_2O_3)$magnetite plus ilmenite. This fractionation factor was derived from Skaergaard data by averaging the data on the B and C liquids and magnetites (Wager and Mitchell, 1951), and using a 1.4 fractionation between ilmenite and magnetite on the melanocratic rock #2308 (Vincent and Phillips, 1954). The latter data agree with that measured on the oxide rich gabbro A408 of the Labrieville massif. A proportion of magnetite to ilmenite of $\frac{1}{4}$ was assumed for the Labrieville crystallization. This procedure amounts to using the vanadium analyses of the magnetites to monitor the crystallization differentiation of vanadium relative to ferric iron assuming that the controlling reaction was the separation of ilmenite. The magnetite analyses are used in preference to the ilmenite analyses because they contain more vanadium, thereby permitting more precise analyses, and because an adjustment factor relating analyses done in Quebec to those done in Japan is available for the magnetites. If the oxide minerals in the Skaergaard are assumed to be recrystallized (all ilmenite derived by oxidation from titaniferous magnetite), then fractionation factors of 0.40 (average of B and C) and 0.50 (B only) are derived. Although there are great uncertainties in the fractionation factor, it is noteworthy that a comparison of the fractionation stages determined by the Rayleigh distillation equation for feldspar and iron-titanium oxides predicts that the residual liquids become enriched in iron-titanium oxide components relative to feldspar components, in qualitative agreement with the observed trend toward rocks rich in iron-titanium oxides and poor in feldspar.

The MnO/FeO ratio of the (hemo-) ilmenites correlates with the V_2O_3/Fe_2O_3 ratio of the coexisting magnetites as shown in Fig. 4. Although most of the manganese is in the iron-titanium oxides, much of it is also in the pyroxenes; therefore, it cannot be easily used to predict the fraction of oxide components crystallized. It is, nevertheless, significant that the Labrieville ilmenites increase in MnO/FeO by a factor of 4.3, whereas the Skaergaard ilmenites increase in MnO/FeO by a factor of only 3.5 (Vincent and Phillips, 1954). This difference suggests that a greater proportion of iron-titanium oxides relative to ferromagnesian silicates were involved in the Labrieville crystallization differentiation than in the Skaergaard, since the fractionation factors for manganese relative to ferrous iron are greater for ilmenite and magnetite than for

ferromagnesian silicates (Wager and Mitchell, 1951). This prediction agrees with the observed high proportion of iron-titanium oxides to pyroxenes in the Labrieville anorthosite massif.

Both the MnO/FeO ratio of the (hemo-) ilmenites and the V_2O_3/Fe_2O_3 ratio of the ilmeno-magnetites show fair correlations with the Fe_2O_3 content of the (hemo-) ilmenites, suggesting the direct influence of the crystallization of the iron-titanium oxide minerals on the trend toward more reducing crystallization conditions during progressive differentiation.[1]

The composition of the hemo-ilmenite comprising the massive hemo-ilmenite deposit at Brule lake in the Labrieville massif is about 30 per cent Fe_2O_3 (Table 5). This composition places the deposit at a fairly early stage in the differentiation of the massif.

(*e*) Pyroxenes. The Fe/(Fe+Mg) ratios of the orthypyroxenes correlate with the other parameters of differentiation as shown on Fig. 4. Using again the data of Wager and Mitchell (1951), stages of crystallization of pyroxene components can be calculated according to the Rayleigh distillation equation. The results are given in Table 11. A comparison with the results based on the barium in the feldspars and the vanadium in the magnetites indicates that the residual liquids became enriched in pyroxene as well as oxides relative to feldspar, and in oxides relative to pyroxenes. The trend toward pyroxene enrichment relative to feldspar is obviously present in the rocks, but the modal data are not adequate to evaluate any persistent trend in enrichment in oxides relative to pyroxenes. The crystallization stages based upon the pyroxenes are probably the least reliable, owing to the possible influence of oxidation-reduction reactions during differentiation and the influence of the oxidizing intensity of the liquid from which the successive pyroxenes crystallized upon their compositions.

(*f*) Apatites. The Eu/Yb, Ce/Y and Cl/(F+Cl) ratios of the analyzed apatites all show negative correlation with the V_2O_3/Fe_2O_3 ratio of the coexisting magnetites (Fig. 4), as would be expected on the basis of the argument that the later apatites should be enriched in the elements with the larger ionic radii. In addition, the later apatites have higher contents of Y+Ce+Eu+Yb.

[1] As may be deduced from the data in Table 5, there is a pronounced dependence of the distribution of vanadium and manganese (as well as aluminum) between (hemo-) ilmenite and ilmeno-magnetite upon the Fe_2O_3 content of the (hemo-) ilmenites. Probably the Fe_2O_3 content of the (hemo-) ilmenites controlled the extent to which the minor elements could enter the ferrian ilmenite lattice during cooling. Also the effect of temperature on the distribution factors may be large. Therefore, the use of the observed MnO/FeO and V_2O_3/Fe_2O_3 ratios to assess differentiation may be misleading to some extent. Since the same trends persist for the total oxide assemblages as for the individual minerals, although to a subdued extent, the qualitative relationships remain the same.

The apatites in the deposit of massive hemo-ilmenite are relatively poor in rare earths and chlorine, indicating the early separation of the deposit.

(*g*) Biotite. The four analyzed biotites span the main part of the differentiation sequence. Their oxy contents, determined by calculation of the unit formula deficiency in OH+F, correlate with the Hm content of the coexisting (hemo-) ilmenites, Fig. 9. The variable oxy contents of the biotites are easily explained in terms of the control of the hyper-solvus hematite-ilmenite solid solutions on the oxygen fugacity of the environment at any particular temperature: the higher the Hm content of the homogenous ferrian ilmenites, the higher the oxygen fugacity developed

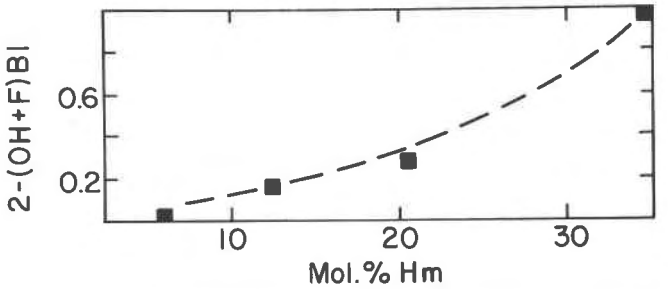

FIG. 9. The oxy content of biotite and the Hm content of coexisting (hemo-) ilmenite.

at any particular temperature, thereby leading to a low OH+F content in the biotite.

Wones and Eugster (1965) have provided a basis for deducing the water fugacity from the composition of biotite in equilibrium with magnetite and potassium feldspar. If it is assumed that the temperature of equilibration lies below that of the beginning of melting of the mineral assemblage containing the biotite, then a maximum water fugacity may be determined for any particular (hemo-) ilmenite and biotite compositions. Since it is reasonable to expect the water fugacity to increase during crystallization, the late stage oxide-rich gabbro, A128, probably crystallized at the highest water fugacity of any of the biotite-bearing rocks. The primary ilmenite in A128 may have been richer in Fe_2O_3 than it is at present; therefore, to allow the highest possible water fugacity an original ilmenite composition of Hm 15 is assumed. A $KAlSi_3O_8$ activity of 0.3 and a Fe_3O_4 activity of 0.7 are assumed. The curve for the beginning of melting of oxidized hawaiite (Yoder and Tilley, 1962) is taken as the most applicable beginning of melting curve for the oxide-rich gabbro. As shown on Fig. 10, the intersection of the temperature, water fugacity curve for A128 biotite coexisting with Hm 15 with the beginning

of melting curve is at about 880° C. and 2000 bars water fugacity. These figures represent the lowest reasonable temperature and highest water fugacity for the biotite-bearing rocks of the Labrieville massif.

The fractionation stage of the feldspars in the oxide-rich gabbro, A128, suggests that the earliest liquid (from which the minerals in A569 noritic anorthosite crystallized) had no more than about 30 per cent as much dissolved water as did the liquid from which the A128 minerals crystallized, assuming the more feldspathic composition compensates for

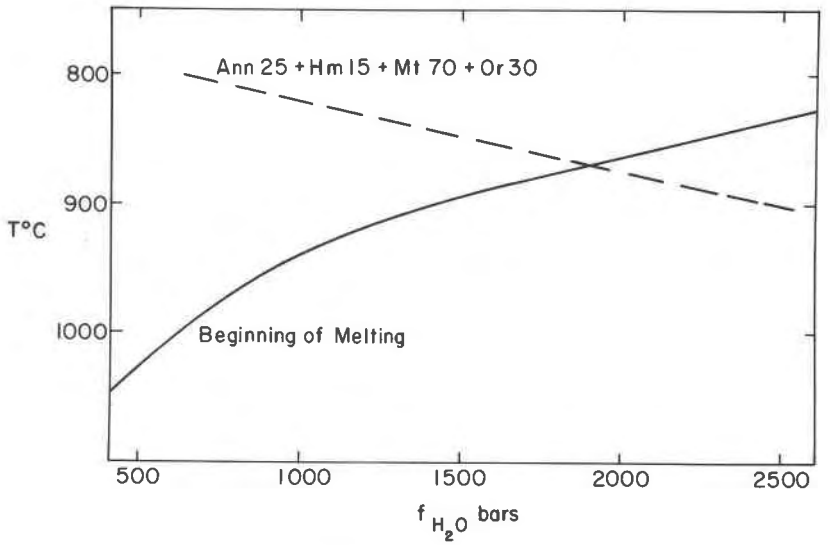

FIG. 10. Temperature—water fugacity relationship of a biotite-bearing assemblage (A128) calculated according to formula 6″ of Wones and Eugster (1965) and the beginning of melting of oxidized hawaiite (from Yoder and Tilley, 1962).

the higher temperature in terms of solubility. The water fugacity of the earliest liquid was therefore no greater than about 500 bars.

SUMMARY OF CONCLUSIONS

Recrystallization

(*a*) Oxidation and reduction. The present compositions of the ilmenomagnetites coexisting with (hemo-) ilmenite suggest that they have experienced granule oxidation exsolution of ferrian ilmenite. The oxidation agent may have been water or the coexisting ferrian ilmenite or a combination of both. In any case, the "exsolved" ilmenite probably had a composition close to that of the coexisting (hemo-) ilmenite, especially in rocks containing appreciable hemo-ilmenite. Only trivial amounts of

the magnetite can have resulted from the oxidation of ortho-pyroxene or the reduction of ferrian ilmenite. In rocks with a high proportion of magnetite to ilmenite, the primary composition of the ilmenite may have been somewhat richer in Fe_2O_3 than it is at present, due to the reducing influence of isocompositional cooling of titaniferous magnetite in the absence of water.

The zoning of hemo-ilmenite and the contrasting compositions of matrix (hemo-) ilmenite and rodlets of hemo-ilmenite and ilmeno-hematite exsolved from plagioclase and antiperthite megacrysts, as well as the correlation between the oxy contents of the biotites and the Fe_2O_3 contents of the coexisting (hemo-) ilmenites, indicate that oxygen fugacity gradients existed at temperatures above the beginning of hematite-ilmenite exsolution.

(*b*) Zoning and exsolution of feldspars. The correlation between the potassium and calcium contents of mesoperthite-rimmed plagioclase megacrysts probably reflects the quantitative influence of the Al/Si ratio of the feldspar ancestor on the rate of exsolution of the two phases. The lower potassium contents of matrix plagioclase are probably due to the influence of physical granulation in promoting exsolution.

The three mm-wide rim of zoned feldspar surrounding the xenoliths of labradorite anorthosite demonstrates the limited extent of redistribution of feldspar constituents during crystallization and cooling of the Labrieville massif.

(*c*) Redistribution of oxygen isotopes. The correlation between the oxygen isotopic composition of the (hemo-) ilmenites and the modal abundance of iron-titanium oxide minerals in the rocks demonstrates that retrograde recrystallization has occurred but that it has been limited in extent.

Crystallization Conditions During Differentiation

(*a*) Temperature. The deduced 2.0 per mil oxygen isotopic fractionation between ilmenite and plagioclase conclusively demonstrates that the primary crystallization of the Labrieville massif took place at very high temperatures similar to or in excess of the 1100° C. characteristic of the crystallization of plagioclase and magnetite (or ilmenite) in basalt.

The high potassium content of the antiperthites in the early rocks and the compositions of coexisting plagioclase and mesoperthite in the later rocks similarly argue for a high temperature of primary crystallization such as would be expected for hawaiite, mugearite and trachyte.

Solidus temperatures of the residual oxide-rich gabbros exceeded about 880° C. as indicated by the composition of biotite.

(*b*) Oxygen fugacity. The compositional change in matrix (hemo-)

ilmenite during differentiation indicates that the residual liquids became reducing relative to the isocompositional cooling curves for ferrian ilmenite, water of constant H_2/H_2O ratio, and even titaniferous magnetite, if the crystallization occurred over a temperature interval of 400° C. or less.

(*c*) Water fugacity. The biotite compositions, viewed in the light of the beginning of melting curve for oxidized hawaiite (Yoder and Tilley, 1963), limit water fugacities of the earliest liquid to less than about 500 bars and of the latest liquid to less than about 2000 bars.

(*d*) Composition. Residual liquids of the Labrieville massif became enriched in BaO/K_2O, Fe_2O_3/V_2O_3, $FeO/FeO+MgO$, MnO/FeO, Cl/F, Ce/Y and Eu/Yb at different rates indicating that the residual liquids either became relatively enriched in iron-titanium oxide and pyroxene components relative to feldspar components, or that the degree of fractional crystallization of iron-titanium oxides and pyroxenes was lower than for feldspars. If any one of the rocks studied can be assumed to be an approximately congruent aliquot of the liquid from which it crystallized, then the composition of the original liquid, from which A569 noritic anorthosite crystallized, can be calculated. The best rock for this purpose is A9b, gabbroic anorthosite, which is massive, uniform and subophitic. Keeping in mind that the feldspar fractionation stage is a minimum based upon a fractionation factor of 0.5, the data on A9b suggest that the earliest liquid was at least 84 per cent feldspar constituents with 5 per cent oxide and 11 per cent pyroxene components. The bulk composition of the massif is 90 per cent feldspars plus or minus about 5 per cent. This close agreement is probably coincidental; nevertheless, it is real and based on only two assumptions: fractionation factors deduced for the Skaergaard intrusion apply to the Labrieville anorthosite; the gabbroic anorthosite, A9b, is a compositionally congruent aliquot of the liquid from which it crystallized.

The Brule Lake Hemo-Ilmenite Deposit

The manganese, vanadium and Fe_2O_3 contents of the hemo-ilmenites and the chlorine and rare earth contents of the apatites in the Brule Lake hemo-ilmenite deposit clearly indicate that the chemical separation of the deposit took place at a very early stage of differentiation.

The iron-titanium oxide deposits in anorthosites have long been regarded by many workers as products of liquid immiscibility. But the prevailing impression, gained from textural and structural observations, has been that they are paragenetically late (Osborne, 1928). The present writer concurs with this textural point of view, but believes that the chemical evidence is so compelling that an hypothesis of early separation

(relative to the crystallization of the whole mass) is required. After early separation the dense, oxide-rich liquid probably intruded the plagioclase mush at the crystal-liquid interface on the floor of the chamber of liquid.

The presence of corundum in the Brule Lake hemo-ilmenite deposit supports the liquid immiscibility hypothesis. At the outset, the two liquids must have been in equilibrium with the same crystalline phases. However, the corundum in the deposit cannot be an equilibrium associate of the quartz in the surrounding anorthosite; according to any hypothesis it must owe its existence to the physical isolation and subsequent crystallization and/or recrystallization of the deposit. The absence of corundum associated with hemo-ilmenite in anorthosite, oxide-rich gabbro and some massive hemo-ilmenite indicates that the corundum is not an exsolution product. The quartz in the perthite-quartz-pyrite pockets is almost certainly the product of late crystallization of trapped liquid. Therefore, it is concluded that the corundum in the hemo-ilmenite deposit is due to the independent crystallization differentiation of the iron-titanium oxide liquid, subsequent to its physical separation from a silicate liquid in which excess silica eventually crystallized.

The early separation of the hemo-ilmenite deposit is expected according to Bowen's (1928) general arguments on liquid immiscibility. Also Fisher (1950) provided an experimental basis for liquid immiscibility between some iron oxide-rich and silicate-rich liquids. In 1961 Park described a magnetite lava flow from Chile. In the writer's judgment the liquid immiscibility hypothesis to account for massive iron-titanium oxide deposits in anorthosites is on very firm ground.

A Note on the Labrieville Aureole

If any appreciable proportion of the crystallization of the Labrieville anorthosite took place in its present structural setting, then large amounts of country rock would have been melted. The several hundred meter thick halo of mafic quartz diorite gneiss, poor in potassium feldspar and quartz but anomalously rich in zircon, is suggestive of a refractory residuum resulting from the partial fusion and selective removal of lowest melting (granitic) constituents. The absence of biotite in (quartz +potassium feldspar+magnetite) gneiss within two kilometers of the anorthosite, stratigraphically, is probably due to either the effect of partial melting by lowering water fugacity, or to higher temperatures near the anorthosite, or a combination of both.

The Origin of the Labrieville Parent Liquid

Previous considerations of the origin of anorthosite parent liquids have primarily focused upon the nearly monomineralic bulk composition

of anorthosite massifs. These attempts, recently summarized by Buddington (1961), Turner and Verhoogen (1960) and added to by Yoder and Tilley (1962, p. 461), are unsatisfactory. Either it is necessary to postulate the existence of genetically associated rocks, for which there is no convincing evidence, or to assume water pressures for which there is no unambiguous field or mineralogical support. This predicament is not alleviated by the findings of the present work, but rather augmented.

The bulk composition of a rock is, of course, an extensive parameter and inherently difficult to treat in termodynamic terms. As a result of the present findings on the Labrieville anorthosite, it is possible to review the origin of the parent liquid in terms of several intensive variables that are essential attributes of the parent liquids of the St. Urbain-type anorthosites.

In the first place, it is clear that the parent liquid was very hot (near or above 1100° C.) and had a fairly low water fugacity (less than 500 bars). Secondly, the parent liquid was uniquely highly oxidizing, and differentiated to produce a relatively reducing residuum. Finally, the liquid was unusually high in Fe+Ti/(Fe+Ti+Mg) and produced an immiscible iron-titanium oxide liquid at an early stage of crystallization. It is difficult to see how such a highly oxidizing liquid could be derived from that part of the mantle which has produced basalts.

Anhydrous partial melting of Lake St. John anorthosite offers an attractive explanation of the highly oxidizing character of St. Urbain type anorthosites. The magnetite and ilmenite now present in the Lake St. John anorthosite have nearly pure end member compositions (work in progress) and are probably present in the average proportion of 60:40 (ilmenite:magnetite) judging from the typical compositions of unoxidized magnetites in massive magnetite deposits in the Lake St. John anorthosite (*e.g.* the LaBlache Lake deposit, work in progress). Simple arithmetic shows that, upon heating, the magnetite and ilmenite would react to give an ilmenite of Hm 33, Il 67 and a magnetite of Mt 50, Usp 50 at about 1200° C. The highly oxidizing character of St. Urbain type anorthosites strongly suggests that they are the products of partial fusion of a previously oxidized rock like the Lake St. John anorthosite.

Acknowledgements

At the suggestion of Marcel Morin, then of the Quebec Department of Natural Resources, I continued the study of the Labrieville anorthosite in 1961 which he had begun in 1953. The early results formed the basis of my Ph.D. dissertation at Princeton University (1963). I continued parts of the study during the tenure of a NSF postdoctoral fellowship at the University of Chicago, where the final analysis was completed

while I was supported by R. N. Clayton through NSF Grant GP2019.

Princeton University and the Quebec Department of Natural Resources supported the cost of chemical analyses. I wish to commend the generosity of field and laboratory support which Quebec provided and particularly to thank Z. Katzendorfer and H. Boileau, the Quebec analysts, for their excellent work upon which much of this study is based.

Although the design of the study is mine, I owe a great debt to many for assistance in interpreting the data: R. B. Hargraves (Princeton University), D. R. Wones and D. B. Stewart (U.S. Geological Survey), D. H. Lindsley (Geophysical Laboratory) and R. N. Clayton (University of Chicago) were especially helpful.

Various stages of the manuscript were read by J. R. Goldsmith and R. N. Clayton of Chicago, A. L. Howland of Northwestern University, R. B. Hargraves and D. B. Stewart whose criticisms resulted in an expansion and almost complete rewriting of the manuscript.

References

Anderson, A. T. and R. N. Clayton (1966) Equilibrium oxygen isotope fractionation between minerals in igneous, meta-igneous and meta-sedimentary rocks. (abs.) *Am. Geophys. Union Trans.* (in press).

—— and M. Morin (1964) Anorthosites in the Grenville of Quebec: a classification. (abs.) *Am. Geophys. Union Trans.* **45,** 125.

Barth, T. F. W. (1951) The feldspar geologic thermometers. *Neues Jahrb. Min. Abhandl.* **82,** 143–154.

—— (1961) The feldspar lattices as solvents of foreign ions. *Spain. Instituto "Lucas Mallada," Cursillos y Conferencias* **8,** 3–8.

Birks, L. S. (1963) *Electron Probe Microanalysis.* Interscience.

Bowen, N. L. (1913) The melting phenomena of the plagioclase feldspars. *Am. Jour. Sci.* (4th ser.) **35,** 577–599.

——— (1928) *Evolution of the Igneous Rocks.* Princeton.

Buddington, A. F. (1939) Adirondack igneous rocks and their metamorphism. *Geol. Soc. Am. Mem.* **7.**

——— (1961) The origin of anorthosite re-evaluated. *Geol. Survey of India, Records* **86,** 421–432.

——— and D. H. Lindsley (1964) Iron-titanium oxide minerals and synthetic equivalents. *Jour. Petrol.* **5,** 310–357.

———, J. Fahey, and S. Vlisidis (1963) Degree of oxidation of Adirondack iron oxide and iron-titanium oxide minerals in relation to petrogeny. *Journ. Petrol.* **4,** 138–169.

Carmichael, C. M. (1961) The magnetic properties of ilmenite-hematite crystals. *Roy. Soc. London Proc.* **263,** 508–530.

Carmichael, I. S. E. (1960) The feldspar phenocrysts of some Tertiary acid glasses. *Min. Mag.* **32,** 587–608.

——— (1963) The crystallization of feldspar in volcanic acid liquids. *Geol. Soc. Lond. Quart. Jour.* **119,** 95–131.

——— (1965) Trachytes and their feldspar phenocrysts. *Min. Mag.* **34,** 107–125.

——— and A. McDonald (1961) The geochemistry of some natural acid glasses from the North Atlantic Tertiary volcanic province. *Geochim. et Cosmochim. Acta* **25,** 189–222.

CLAYTON, R. N. AND T. K. MAYEDA (1963) The use of bromine pentafluoride in the extraction of oxygen from oxides and silicates for isotopic analysis. *Geochim. et Cosmochim. Acta* **27,** 43–52.

COMPSTON, W. AND S. EPSTEIN (1958) A method for the preparation of carbon dioxide from water vapor for oxygen isotopic analysis. (abs.) *Am. Geophys. Union Trans.* **39,** 511–512.

CRAIG, H. (1957) Isotopic standards for carbon and oxygen and correction factors for mass-spectrometric analysis of carbon dioxide. *Geochim. et Cosmochim. Acta* **12,** 133–149.

——— (1961) Standard for reporting concentrations of deuterium and oxygen-18 in natural waters. *Science* **133,** 1833–1834.

DALY, R. A. (1933) *Igneous Rocks and the Depths of the Earth.* McGraw-Hill Book Co., Inc., New York.

EMMONS, R. C. (1953) Selected petrogenic relationships of plagioclase. *Geol. Soc. Am. Mem.* **52.**

FISCHER, R. (1950) Entmischungen in Schmelzen aus schwermetall Oxygen, Silikaten, und Phosphaten. Ihre geochemische und lagerstattenkundliche Bedeutung. *Neues Jahrb. Mineral. Abh.* **81,** 315–364.

GOLDSCHMIDT, V. M. (1954) *Geochemistry.* Oxford.

GOLDSMITH, J. R. AND F. LAVES (1954) Potassium feldspars structurally intermediate between microcline and sanidine. *Geochim. et Cosmochim. Acta* **6,** 100–118.

GUNN, B. M. (1965) K/Rb and K/Ba ratios of Antarctic and New Zealand tholeiites and alkali basalts. *Jour. Geophys. Res.* **70,** 6241–6247.

HARGRAVES, R. B. (1962) Petrology of the Allard lake anorthosite suite, Quebec. *Geol. Soc. Buddington Vol.,* 163–189.

HESS, H. H. (1960) Stillwater igneous complex, Montana. *Geol. Soc. Am. Mem.* **80.**

HOWIE, R. A. (1955) The geochemistry of the charnockite series of Madras, India. *Roy. Soc. Edin. Trans.* **62,** 725–768.

MAWDSLEY, J. B. (1927) St. Urbain area, Charlevoix district, Quebec. *Geol. Survey Can. Mem.* **152.**

MCKINNEY, C. R., J. M. MCCREA, S. EPSTEIN, H. A. ALLEN AND H. C. UREY (1950) Improvements in mass spectrometers for the measurement of small differences in isotopic abundance ratios. *Rev. Sci. Instr.* **21,** 724–730.

MICHOT, P. (1939) Les anorthosites de la region d'Egersund (Norvege). *Acad. Royale Belgique Bull., Class Sci.* (5 ser.) **25,** 491–503.

MORIN, M. (1956) Geology of the Labrieville map area, Saguenay County, Quebec. Ph.D. Diss., Laval Univ.

MUIR, I. D. AND J. V. SMITH (1956) Crystallization of feldspars in larvikite. *Zeit. Krist.* **107,** 182–195.

——— AND C. E. TILLEY (1961) Mugearites and their place in alkali igneous rock series. *Jour. Geol.* **69,** 186–203.

MUAN, A. AND E. F. OSBORN (1956) Phase equilibria at liquidus temperatures in the system MgO-FeO-F_2O_3-SrO_2. *Am. Ceram. Soc. Jour.* **39,** 121–140.

NEWHOUSE, W. H. (1936) Opaque oxides and sulphides in common igenous rocks. *Geol. Soc. Am. Bull.* **47,** 1–52.

NIER, A. O. C. (1947) A mass spectrometer for isotope and gas analysis. *Rev. Sci. Instr.* **18,** 398–411.

OSBORNE, F. F. (1928) Certain magmatic titaniferous iron ores and their origin. *Econ. Geol.* **23,** 724–761, 895–922.

PAPEZIK, V. S. (1965) Geochemistry of some Canadian anorthosites. *Geochim. et Cosmochim. Acta* **29,** 673–710.

PARK, C. F., JR. (1961) A magnetite flow in northern Chile. *Econ. Geol.* **56,** 431–435.

SEN, S. K. (1959) Potassium content of natural plagioclases and the origin of antiperthites. *Jour. Geol.* **67,** 479–495.

——— (1960) Some aspects of the distribution of barium, strontium, iron and titanium in plagioclase feldspars. *Jour. Geol.* **68,** 638–665.

SMITH, J. R. AND H. S. YODER (1956) Variations in *x*-ray powder diffraction patterns of plagioclase feldspars. *Am. Mineral.* **41,** 632–647.

SMITH, J. V. AND P. GAY (1958) The powder patterns and lattice parameters of plagioclase feldspars, II. *Min. Mag.* **31,** 744–762.

TAYLOR, H. P. AND S. EPSTEIN (1963) $0/^{1}$ 0^{16} ratios in rocks and co-existing minerals of the Skaergaard intrusion, east Greenland. *Jour. Petrol.* **4,** 51–74.

TAYLOR, R. W. (1964) Phase equilibria in the system FeO-Fe_2O_3-Tio_2 at 1300°C. *Am. Mineral.* **49,** 1016–1030.

TURNER, F. J. AND J. VERHOOGEN (1960) *Igneous and Metamorphic Petrology* (2 ed.). McGraw-Hill Book Co., Inc., New York.

VINCENT, E. A. AND R. PHILLIPS (1954) Iron-Titanium oxide minerals in layered gabbros of the Skaergaard intrusion, east Greenland. *Geochim. et Cosmochim. Acta* **6,** 1–26.

WAGER, L. R. (1960) The major element variation of the layered series of the Skaergaard intrusion and a re-estimation of the average composition of the hidden layered series and of the successive residual magmas. *Jour. Petrol.* **1,** 364–398.

——— AND R. L. MITCHELL (1951) The distribution of trace elements during strong fractionation of basic magma—a further study of the Skaergaard intrusion, east Greenland. *Geochim. et Cosmochim. Acta* **1,** 129–208.

WAGMAN, D. D., J. E. KILPATRICK, W. J. TAYLOR, K. S. PITZER AND F. D. ROSSINI (1945) Heats, free energies and equilibrium constants of some reactions involving O_2, H_2, H_2O, C, CO, CO_2 and CH_4. *U.S. Nat. Bur. Stds. Jour. Res.*, **34,** 143–162.

WALKER, F., H. C. C. VINCENT, AND R. L. MITCHELL (1952) The chemistry and mineralogy of the Kinkell tholeiite, Stirlingshire. *Min. Mag.* **29,** 895–908.

WEBSTER, A. H. AND N. F. H. BRIGHT (1961) The system iron-titanium-oxygen at 1200°C. and oxygen partial pressures between 1 atm. and 2×10^{-14} atm. *Amer. Ceram. Soc. Jour.* **44,** 110–116.

WONES, D. R. AND H. P. EUGSTER (1965) Stability of biotite: experiment, theory and application. *Am. Mineral.* **50,** 1228–1272.

WRIEDT, H. A. AND J. CHIPMAN (1956) Oxygen in liquid iron-nickel alloys. *Am. Inst. Min. Met. Pet. Eng. Trans.* (*Jour. Metals*) **206,** 1195–1199.

YODER, H. S., D. B. STEWART, AND J. R. Smith (1957) Ternary feldspars. (*Ann. Rep. Dir. Geophys. Lab.*) *Carnegie Inst. Washington Yr. Book* **56,** 206–214.

——— AND C. E. TILLEY (1962) Origin of basalt magmas: an experimental study of natural and synthetic rock systems. *Jour. Petrol.* **3,** 342–532.

Manuscript received, March 6, 1966; accepted for publication May 5, 1966.